NASA TECHNICAL MEMORANDUM

NASA TM X-68225

NASA TM X-68225

PRELIMINARY INVESTIGATION OF INLET INGESTION OF A WING TIP VORTEX

by Glenn A. Mitchell
Lewis Research Center
Cleveland, Ohio 44135
April, 1973

ABSTRACT

An inlet-coldpipe assembly was placed in a Mach 0.4 stream to ingest the tip vortex of a forward mounted wing. The strongest vortex was produced by a wing angle of attack of 11 degrees. The vortex displayed a tangential velocity of 57 percent of local stream velocity prior to entering the inlet, and a tangential velocity of 25 percent of local velocity at the simulated compressor-face. The total-pressure profiles measured by standard compressor-face rakes were changed by the presence of the vortex only at the highest tested inlet mass-flow ratios.

E-7428

PRELIMINARY INVESTIGATION OF INLET INGESTION OF A WING TIP VORTEX

by Glenn A. Mitchell

Lewis Research Center

SUMMARY

An inlet-coldpipe assembly was placed in a Mach 0.4 stream in the Lewis 10- by 10-Foot Supersonic Wind Tunnel and ingested the tip vortex of a forward mounted wing. The vortex was surveyed with flow angularity probes prior to its entering the inlet. Probes were also fixed at the simulated compressor face to detect the vortex within the inlet. The effect of the vortex was also measured by standard compressor-face total-pressure rakes.

Measurements at the maximum inlet mass-flow ratio revealed that the vortex reached the compressor-face station with a maximum tangential velocity of 25 percent of local axial velocity. This vortex was the strongest and was produced by a wing angle of attack of 11 degrees. Prior to entering the inlet, the maximum tangential velocity was 57 percent of local stream velocity. The vortex changed the compressor-face total-pressure profiles only at the highest tested inlet mass-flow ratio. Near the inlet entrance, the vortex path was changed from its expected position by the airflow that was deflected and spilled by the inlet.

E-7428

INTRODUCTION

Some aircraft require the use of forward mounted stub wings for stability and control purposes. At large angles of attack such a wing would generate a strong tip vortex. It is probable that certain combinations of airplane pitch and yaw would cause the vortex to trail aft into an engine air inlet. The effects of such a vortex on engine operating

characteristics are unknown but may be degrading enough to cause engine stall.

A preliminary study of some of these phenomena was conducted in the Lewis 10- by 10-Foot Supersonic Wind Tunnel with the test section operating at a subsonic speed of Mach 0.4. Reynolds number was 7.5×10^6 per meter. A wing was mounted in the test section forward of an inlet-coldpipe combination so that the tip vortex trailed aft into the inlet. A rake of flow angularity probes mounted forward of the inlet was used to analyze the nature of the created vortex prior to its entering the inlet. The inlet was operated over a range of mass-flow ratios both with and without the vortex present to determine its effects on standard compressor-face total-pressure rakes. The rake of flow angularity probes was installed at the compressor-face station for part of the test to detect the nature of the vortex after passing through the inlet.

U.S. Customary Units were used in the design of the test model and for the recording and computing of experimental data. These units were converted to the International System of Units for presentation in this report.

SYMBOLS

b	wing span, cm
c	wing tip chord, cm
H	annulus height at compressor face station, cm
h	distance from hub surface, cm
m_i/m_o	inlet mass-flow ratio
P	total pressure, N/m^2
P_0	free stream total pressure, N/m^2
P_2	compressor face station total pressure, N/m^2

u_n velocity normal to the flow angularity rake, m/sec

u_y velocity in the spanwise direction, m/sec

u_2 local axial velocity at compressor face station, m/sec

v_0 local stream axial velocity, m/sec

x streamwise (axial) ordinate, aft from wing tip

y spanwise ordinate, outboard from wing tip

y_c spanwise location from vortex center, cm

z normal ordinate, above upper wing surface from wing tip trailing edge

z_c normal (to wing) location from vortex center, cm

α inlet angle of attack

APPARATUS AND PROCEDURE

The inlet used in this investigation was a two-dimensional, internal-compression type designed for operation at a Mach number of 2.2. The inlet was attached to a cylindrical nacelle 0.635 meter in diameter in which a J85-13 engine or a cold-pipe choked-exit plug assembly could be installed. For this study, only the cold-pipe assembly was used. The inlet - cold-pipe assembly, as mounted in the tunnel test section, is shown in figure 1. The inlet height (ramp edge to cowl lip) was 0.408 meter and the ramp width was 0.369 meter.

Although the selection of the inlet model was based primarily upon availability, the inlet is an excellent one for a basic study of vortex effects within the inlet at the diffuser exit (compressor face). This is because of the relative openness of the inlet and the lack of protruding surfaces or sharp diffuser turns that might cause the entering vortex to burst.

The inlet geometry was varied by movable ramps. The first ramp was a fixed one, having an angle of 3 degrees with the inlet at zero degrees angle of attack. The second and third ramps were variable and

together with the first ramp accomplished external compression during supersonic operation. The last and fourth ramp was a backward facing ramp which initiated internal flow diffusion. For this test the inlet throat area was opened to a maximum by setting the ramps as flat as possible. The resulting second and third ramp angles of $5\frac{1}{3}$ and $7\frac{2}{3}$ degrees are shown in figure 1. A bleed slot between the third and fourth ramp was available for boundary layer control. All bleed and bypass systems were closed for this test.

Three basic variations exist between the inlet configuration shown in the figure and the configuration actually used during the test. The vortex generators shown in figure 1 on the ramp and side walls were not present for this test. Also the side fairings were not cut back as in figure 1 but extended straight from the ramp edge to a point just above the cowl lip. The cowl lip was not sharp as shown but was 0.76 centimeters thick and blunted with a 3 to 1 ellipse.

The wing used to create the tip vortex was fashioned from an existing strut. Details of the wing are shown in figure 2. The wing had a slight aft sweep of the leading edge and a forward sweep of the trailing edge. Also, the wing was symmetrical, with parallel upper and lower surfaces over much of the chord. The leading edge was a 4.52 to 1 ellipse and the trailing edge was formed by a 25 degree included angle and faired into the straight sides of the wing.

The relation of the wing to the inlet is shown in figure 3. Figure 4 shows details of the test configuration. The wing was mounted forward of the inlet and extended vertically down from the tunnel ceiling. The inlet was located aft of the wing with the ramp edge 8.2 wing-tip chord lengths downstream of the wing-tip trailing edge. By pitching the inlet-coldpipe nacelle to various angles of attack, the inlet entrance was placed at various vertical locations relative to the vortex trailing aft from the wing. As indicated in figure 4, positive angle of attack was opposite to the normal convention. This was because the inlet was mounted upside down in the tunnel.

During part of the test program, a rake of flow angularity probes was mounted in front of the inlet as shown in figure 4. The vertical location of the rake was 20.3 centimeters above the ramp edge. This placed the rake on the inlet horizontal centerline at 0 degree angle of attack. The rake was placed 30.48 centimeters forward of the ramp leading edge as shown in figure 5. The lateral location of each flow angularity probe on the rake is shown in the figure. Each probe consisted of three 0.084 centimeter outside diameter stainless-steel tubes which were soldered adjacent to each other in a vertical plane. The top and bottom tubes were cut at a 45-degree angle as shown. Each probe was calibrated in a special test rig at Mach 0.4 at pitch angles from -35 to +35 degrees. The effect of yaw flow angles on the pitch plane calibration was not determined for each probe. According to reference 1, a yaw flow of 30 degrees causes up to a 4 degree error in the pitch calibration. For the current test such errors were not considered important because credence was given to the measured flow angles only when the rake was near the vortex center where little yaw flow existed.

Total-pressure rakes at the simulated compressor face were installed primarily in the right hand side of the duct, as shown in figure 6. Estimates of the vortex path from references 2 to 4 would place the vortex on this side of the duct. The expected horizontal displacement of the vortex is shown in the figure. Total-pressure rakes 1 to 6, which were area weighted, were used in conjunction with the hub and tip static pressures to compute the inlet mass-flow ratio. The rake of flow angularity probes was, for a part of the test, installed at the compressor face at the circumferential position shown in figure 6. Because of mounting problems only six of the probes could be placed in the duct.

The initial part of the test program was conducted to obtain the strongest vortex from the wing. This goal was attained by testing with the wing at various angles of attack and surveying the created vortex with the rake of flow angularity probes mounted forward of the inlet (fig. 4).

With the wing set at the angle yielding the strongest vortex, the rake was removed, allowing the vortex to trail undisturbed into the inlet. The vertical position of the vortex relative to the compressor face was varied by setting different inlet pitch angles. This procedure placed the vortex at various positions along the vertical centerline shown in figure 6. (Two positions of the vortex are shown as a visualization aid.) The effects of the vortex on the standard compressor face rakes were determined by comparing the data obtained during the above procedure with data obtained when the vortex was not present. Data of this type was obtained at various inlet mass-flow ratios. The maximum mass flow through the inlet was obtained by removing the cold pipe assembly from the inlet. This action also removed the attached compressor face hub. It was at this condition of maximum mass flow that the rake of flow angularity probes was installed in the compressor face (fig. 6) to detect the vortex at this station.

The vortex data obtained during the test were related to the wing geometry by the use of the coordinate system shown in figure 7. The local vortex flow angles that were measured by the flow angularity probes were converted to the tangent of each angle and presented as a local velocity ratio.

RESULTS AND DISCUSSION

The results of varying the wing angle of attack to obtain the strongest vortex are presented in figure 8. Each point on the plot represents the maximum tangential velocity, at an x/c of 7.03, produced by the trailing vortex at a particular wing angle of attack. Each point was obtained from a survey such as presented in figure 9. Obviously, the strongest vortex was produced by a wing angle of attack near 11 degrees. The maximum tangential velocity of the vortex at this streamwise station was recorded as 57 percent of the local stream velocity. The local stream velocity is known to vary across the vortex core region. Both increases and decreases in axial velocity have been reported (refs.

2 and 3, e.g.). Since the maximum changes in the axial velocity generally occur at the core center, the local axial velocity at the core edge is probably no more than a few percent different from the free stream axial velocity. Thus it is significant that the recorded tangential velocity of 57 percent of local stream velocity is larger than values reported in references 2 to 4 where the maximum tangential velocity in the vortex ranged from 10 to 40 percent of the free stream velocity at an x/c of 7.

The results of the flow angularity rake survey across the vortex produced by the wing at 11 degrees angle of attack are shown in figure 9. The spanwise velocity, recorded by each probe as a flow angle, is plotted at the probes normal coordinate position for each spanwise position of the rake. From this figure it was estimated that the spanwise position of the vortex center was at an y/c position of -0.275. The estimate was made by assuming that the center of the vortex would be at the rake spanwise position having the maximum indicated normal velocity slope. At rake spanwise position near -0.275(y/c), the normal coordinate of the vortex center was picked as 0.22 (z/c); the point where the velocity distributions cross zero. The diameter of the vortex core was estimated from figure 9 to be 0.17 tip chords. The core diameter was defined as the distance across the vortex center, measured from the maximum tangential velocity on one side to the maximum tangential velocity on the other side. (With the rake positioned at the core center, the measured spanwise velocity was the tangential velocity.)

The results obtained from the flow angularity rake ($x/c \approx 7$) are compared in figure 10 to data obtained by other investigators (refs. 2 to 4). These data were obtained using rectangular wings and known airfoil shapes as noted in the figure. The path of the vortex of the current test, as revealed by the rake survey at $x/c \approx 7$, agrees quite well in the spanwise plane with those shown in the figure for references 2 to 4. The agreement is not as good in the normal axis, however, with the vortex of the present test trailing higher above the wing than the others. The tabu-

lation of vortex core diameter in figure 10 indicates that the core size determined from the current test is a reasonable value.

Also shown in figure 10 are spanwise vortex center positions at axial locations of 10 and 12.3 (x/c). These data show the vortex path to be greatly altered from the path reported by other investigators. The data were obtained from a schlieren photograph of the vortex path with the inlet model drooped below the vortex at 11.3 degrees. Although the inlet centerline at the ramp edge was 2.8 wing tip chord lengths outboard of the wing, the flow around the model greatly influenced the vortex path as shown in the figure. The schlieren photograph is shown in figure 11. The vortex path is clearly shown by the density gradient across the core region.

By analyzing a series of schlieren photographs such as was shown in figure 11, the effect of the spanwise position of the inlet on the vortex path was determined (fig. 12). The inlet was pitched to various angles, changing inlet spanwise positions, in the vicinity of the wing trailing edge. The vortex center location at $x/c = 10$ was determined for each position; x/c of 10 was just downstream of the schlieren window upstream edge (fig. 4). Figure 12 shows that the spanwise vortex center location did not significantly vary with the inlet spanwise location. Also, figure 12 shows that a change in the inlet mass-flow ratio affected the vortex path. An increase in inlet flow spillage caused the vortex path to bend inboard. This might be expected because of the orientation of the two-dimensional inlet which directed spilled flow in the inboard direction. The effect of inlet mass-flow ratio, or spillage, on the vortex path near the cowl lip is strikingly illustrated by the schlieren photographs presented in figure 13.

The total pressures across the vortex core region at $x/c \approx 7$ were measured by the flow angularity probes. The indicated total-pressure recoveries for two planes of survey through the core are presented in figure 14. A spanwise survey plane is shown at the top of the figure and its distance from the vortex core centerline is shown by the diagram in the center of the figure. The bottom of the figure presents the recoveries measured in a plane normal to the wing and nearly through the vortex

core center. As shown in the figure, the pressure profile across the core is symmetrical in the spanwise direction but somewhat unsymmetrical to the core center in the normal direction. The total pressure in the core center was only 91 percent of the free stream total pressure. The loss of total pressure in the vortex core is also mentioned in references 5 and 6. Reference 6 supposes that the loss is a result of the profile drag losses on the wing. The low energy wake air rolls up with the vortex and follows the axial vortex lines to concentrate the low energy air along the vortex axis. The pressure data in figure 14 also indicate a loss of total pressure at the core edge and beyond. This data is probably in error because the probes are known to indicate erroneously low pressures at high incident flow angles; typically about 2.5 percent pressure loss at the 30 degree incidence angle of the rotating flow at the core edge. Thus only the pressures near the core center were reasonably accurate.

Figure 15 presents the compressor-face station total-pressure rake profiles that were obtained with and without the vortex trailing aft into the inlet. These data were obtained at an inlet mass-flow ratio of 0.63. The presence of the vortex did not significantly affect the measured pressure profiles. The standard pressure instrumentation would not detect the vortex at these conditions. In figure 15(a) the vortex center approached the inlet near the cowl lip; in fact, the core missed entering the inlet as shown in figure 13(b). For figure 15(b) the inlet was pitched up in the test section so that the vortex entered the inlet. Because of this pitch up the entering vortex could not be seen at the forward edge of the schlieren window. The cowl lip area was visible and revealed no evidence of the vortex spilling overboard.

Figure 16 presents the compressor-face station total-pressure profiles obtained at the maximum inlet mass-flow ratio. As noted in the APPARATUS AND PROCEDURE section of this report the maximum mass flow was obtained by removing the inlet cold pipe assembly. This action also removed the simulated compressor hub. Although the hub was gone, the data of figure 16 is plotted from hub to tip in the same manner as figure 15. Each part of figure 16 compares total pressures obtained with

and without the entering vortex. Parts (a) through (j) of the figure show pressure profiles for different vortex positions relative to the inlet. In part (a), for example, the vortex was entering the inlet almost impinging on the cowl lip; whereas in part (j) the vortex was near the inlet centerline.

As figure 16 illustrates, the presence of the vortex significantly changed the compressor-face station total-pressure profiles near the top of the duct at this higher mass-flow ratio of 0.86. Without the entering vortex, the pressure profiles indicate that the upper part of the duct contained a large region of relatively low energy air. It appears that the action of the vortex was to energize this retarded flow region. This action appears similar to that induced by small vortices created by diffuser mounted vortex generators. They are reported in reference 7 to be capable of energizing retarded flow regions in a diffuser. The lack of effect of the vortex at the lower mass-flow ratios (fig. 15) may be due to the lack of low energy regions at the compressor face. However, the probability exists that the vortex was severely weakened or suffered burst before reaching the compressor face at the lower mass-flow ratios.

At the highest mass flow ratio, the entering vortex had not burst and was still relatively strong at the compressor face. Figure 17 presents data from the flow angularity rake which was installed at the compressor-face station as shown in figure 6. Part (a) through (j) of the figure show the same spanwise inlet positions as were shown in figure 16. The progressive profile changes in figure 17 with the vortex present, suggest that the vortex was near the top of the compressor face with the inlet at $y/c = 0.474$ and moved vertically toward the inlet center as the inlet y/c was progressively changed to $y/c = -0.433$. With the inlet centerline at $y/c = 0.474$, the location of the vortex near the top of the duct caused the tangential flow of the vortex to be in line with the flow angularity rake and at right angles to the flow sensing direction of the probes. Thus no flow angle or normal velocity is detected. As the inlet was moved, and the vortex proceeded downward, the vortex axis

became increasingly alined with the rake and the tangential flow of the vortex became increasingly lined up with the flow sensing direction of the probes. The best alinement appears to be with the inlet at $y/c = 0.320$. The profiles of the flow angularity rake near this inlet position suggest that the vortex axis was located to the left of the rake toward the duct center. The maximum normal velocity measured at the inlet y/c of 0.320 indicated that the maximum vortex tangential velocity at the compressor face station ($x/c = 18.2$) was probably in excess of 25 percent of the local axial velocity.

SUMMARY OF RESULTS

An inlet-coldpipe assembly was placed in a Mach 0.4 stream in the Lewis 10- by 10-Foot Supersonic Wind Tunnel so as to ingest the tip vortex of a wing mounted at a forward location in the test section. The vortex was surveyed with a rake of flow angularity probes prior to its entering the inlet. To detect the vortex within the inlet this rake was also mounted at a fixed location at the simulated compressor face. Some effects of the vortex on standard compressor face station total-pressure rakes were determined. The following results were obtained:

1. The vortex was detected at the compressor-face station. (Measurements were made only at conditions of maximum mass-flow ratios.) It had not burst and was still strong with a maximum tangential velocity in excess of 25 percent.

2. The vortex changed the compressor-face total-pressure profiles but only at the highest inlet mass-flow ratios. The effect seemed due to the ability of the vortex to energize a region of retarded flow.

3. The strongest vortex was produced by the wing at 11 degrees angle of attack. Prior to entering the inlet, the vortex produced a maximum tangential velocity of 57 percent of free stream velocity. The vortex core diameter was 1.7 wing tip chords. A core total-pressure loss of 9 percent was measured.

4. The initial path of the vortex as it trailed aft from the wing was in good agreement with paths noted by other investigators. In the vicinity of the inlet, however, the vortex path was changed from that expected in undisturbed flow by the airflow that was deflected and spilled by the inlet.

REFERENCES

1. Dudzinski, Thomas J.; and Krause, Lloyd N.: Flow-Direction Measurement with Fixed-Position Probes. NASA TM X-1904, 1969.

2. Fage, A.; and Simmons, L. F. G.: An Investigation of the Air-Flow Pattern in the Wake of an Aerofoil of Finite Span. Phil. Trans. Roy. Soc. (London), Ser. A. vol. 225, no. 632, Dec. 7, 1925, pp. 303-330.

3. Chigier, N. A.; and Corsiglia, V. R.: Wind-Tunnel Studies of Wing Wake Turbulence. J. Aircraft, vol. 9, no. 12, Dec. 1972, pp. 820-825.

4. Dosanjh, D. S.; Gasparek, E. P.; and Eskinazi, S.: Decay of a Viscous Trailing Vortex. Aeron. Quart., vol. 13, Pt. 2, May 1962, pp. 167-188.

5. Newman, B. G.: Flow in a Viscous Trailing Vortex. Aeron. Quart., vol. 10, Pt. 2, May 1959, pp. 149-162.

6. Brown, Clinton E.: On the Aerodynamics of Wake Vortices. Tech. Rep. 7115, Hydronautics, Inc. (AFOSR-72-1209TR, AD-744860), May 1972.

7. Mitchell, Glenn A.; and Davis, Ronald W.: Performance of Centerbody Vortex Generators in an Axisymmetric Mixed-Compression Inlet at Mach Numbers from 2.0 to 3.0. NASA TN D-4675, 1968.

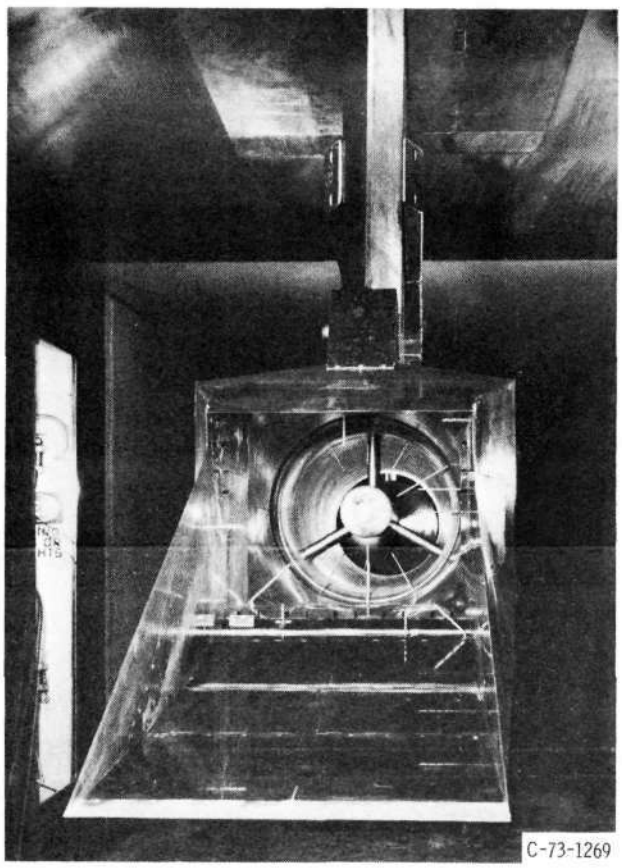

Figure 1. - Inlet model installed in 10- by 10-Foot Supersonic Wind Tunnel.

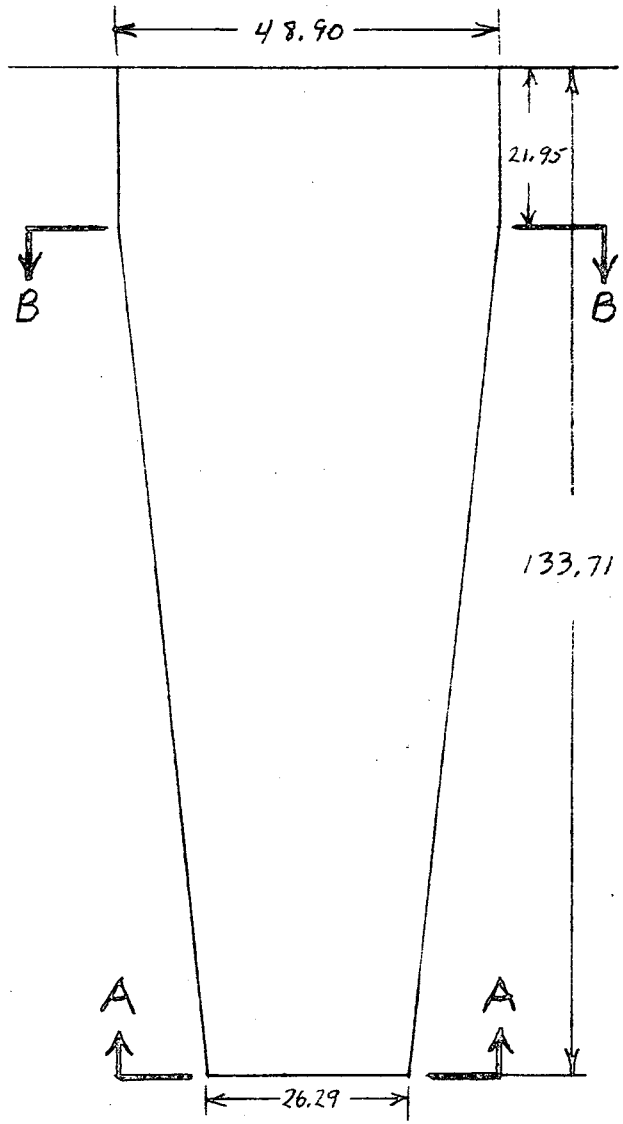

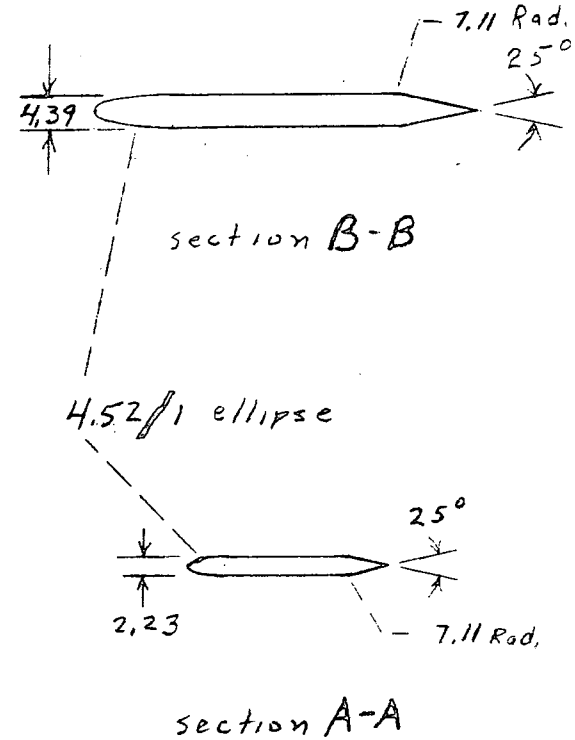

Figure 2.- Details of wing (All dimensions are in centimeters).

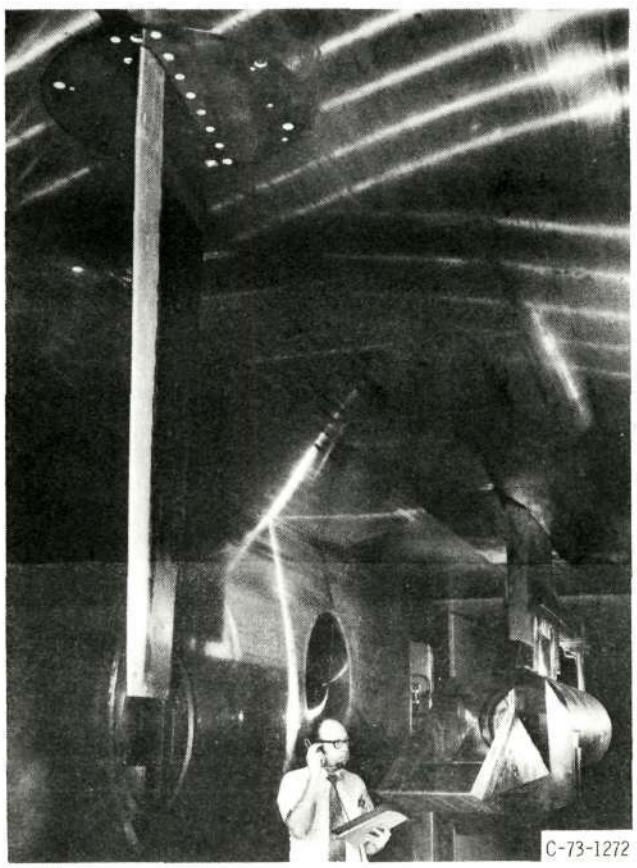

Figure 3. - Wing and inlet installed in 10- by 10-Foot Supersonic Wind Tunnel.

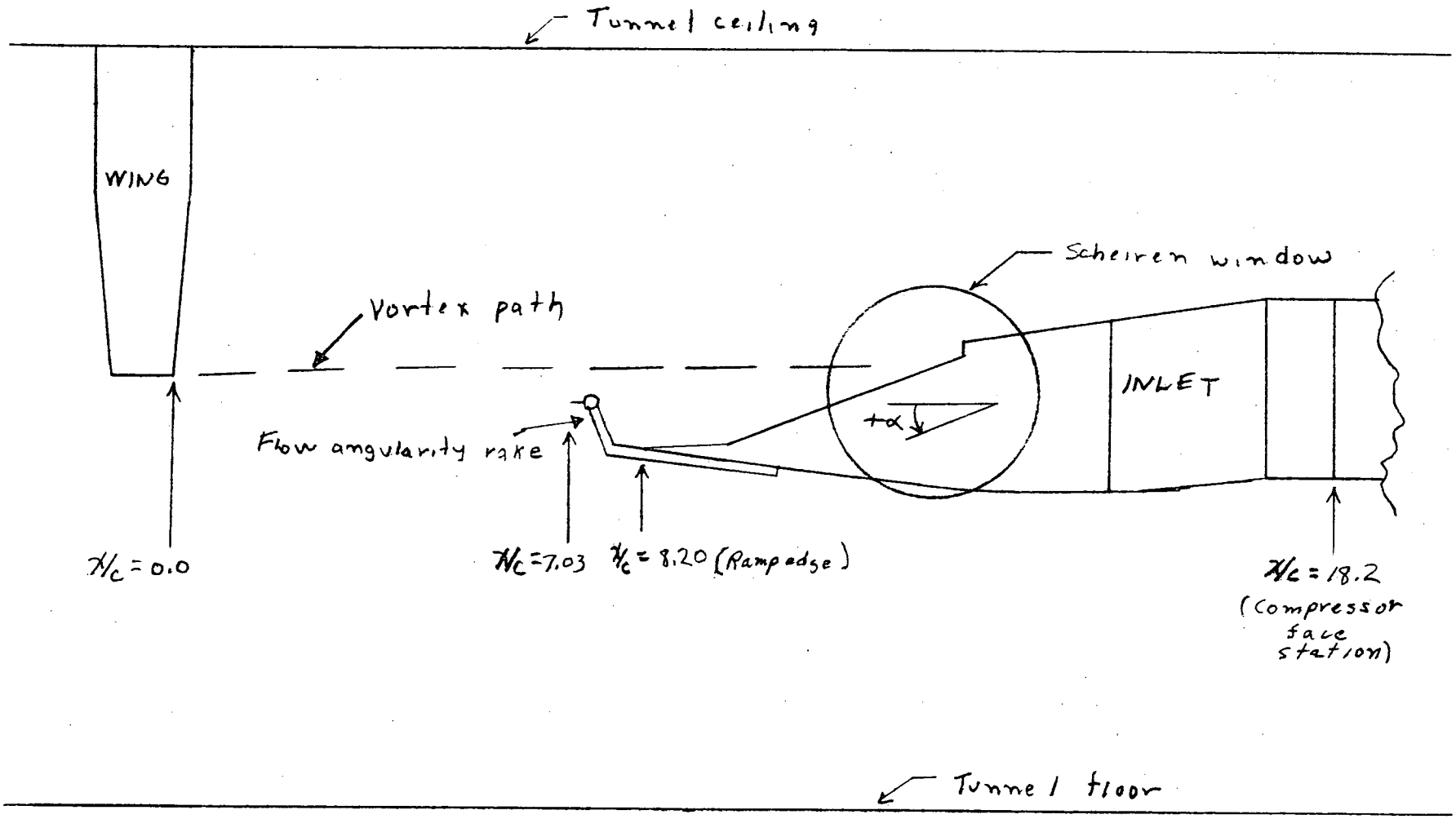

Figure 4. - Schematic of test set up

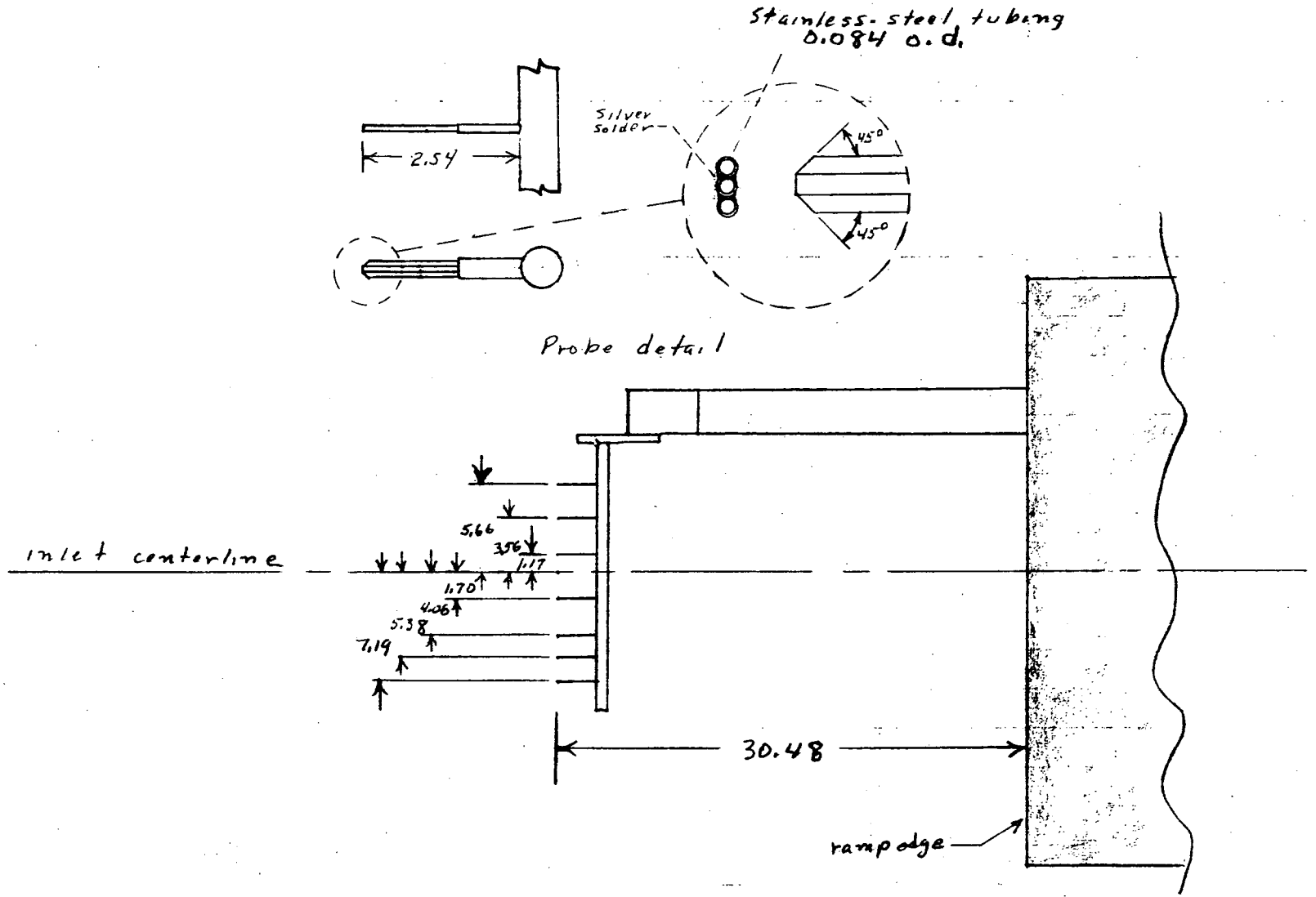

Figure 5. - Planview of flow angularity rake installation (All dimensions in centimeters).

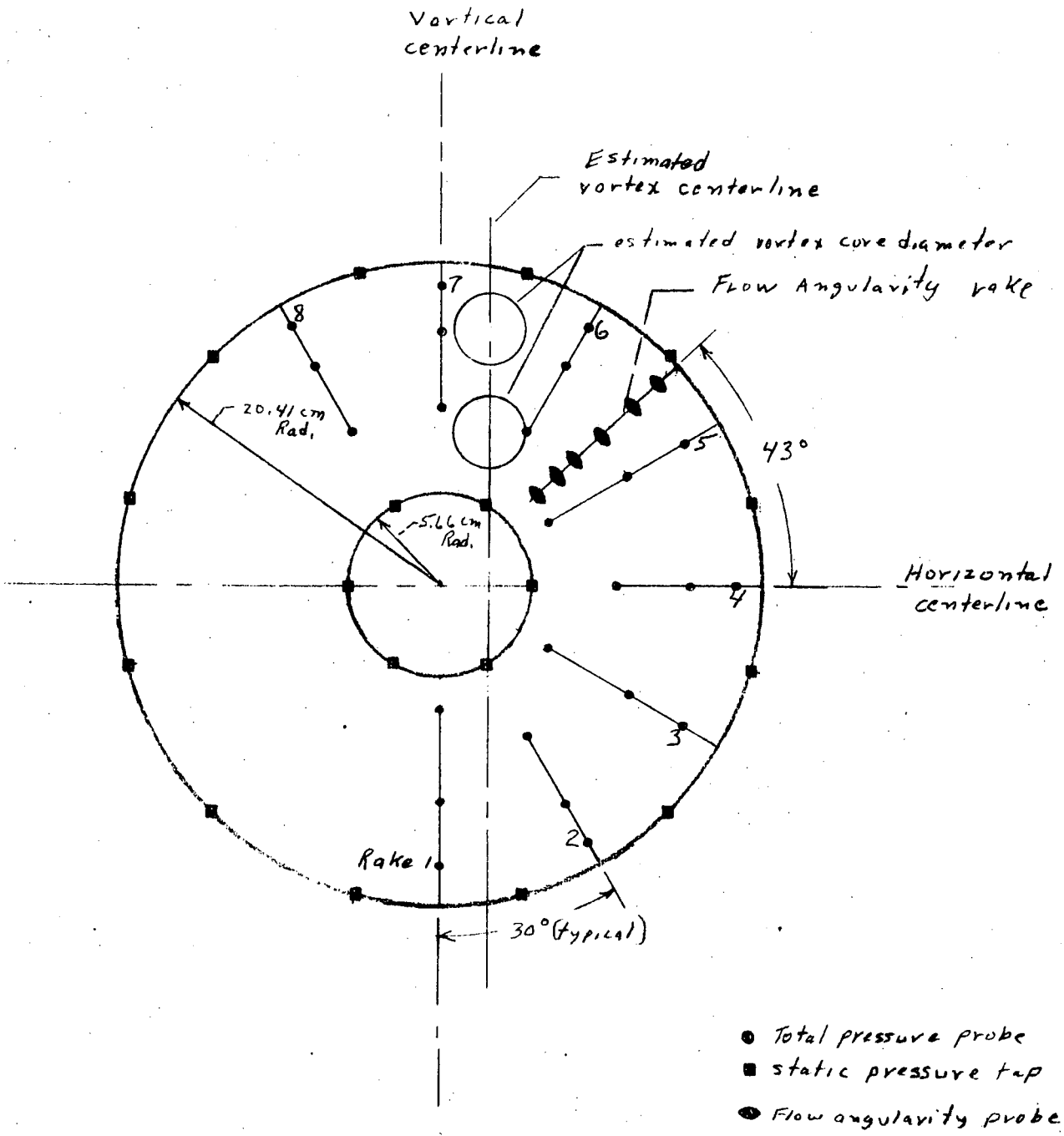

Figure 6. - Compressor face instrumentation.

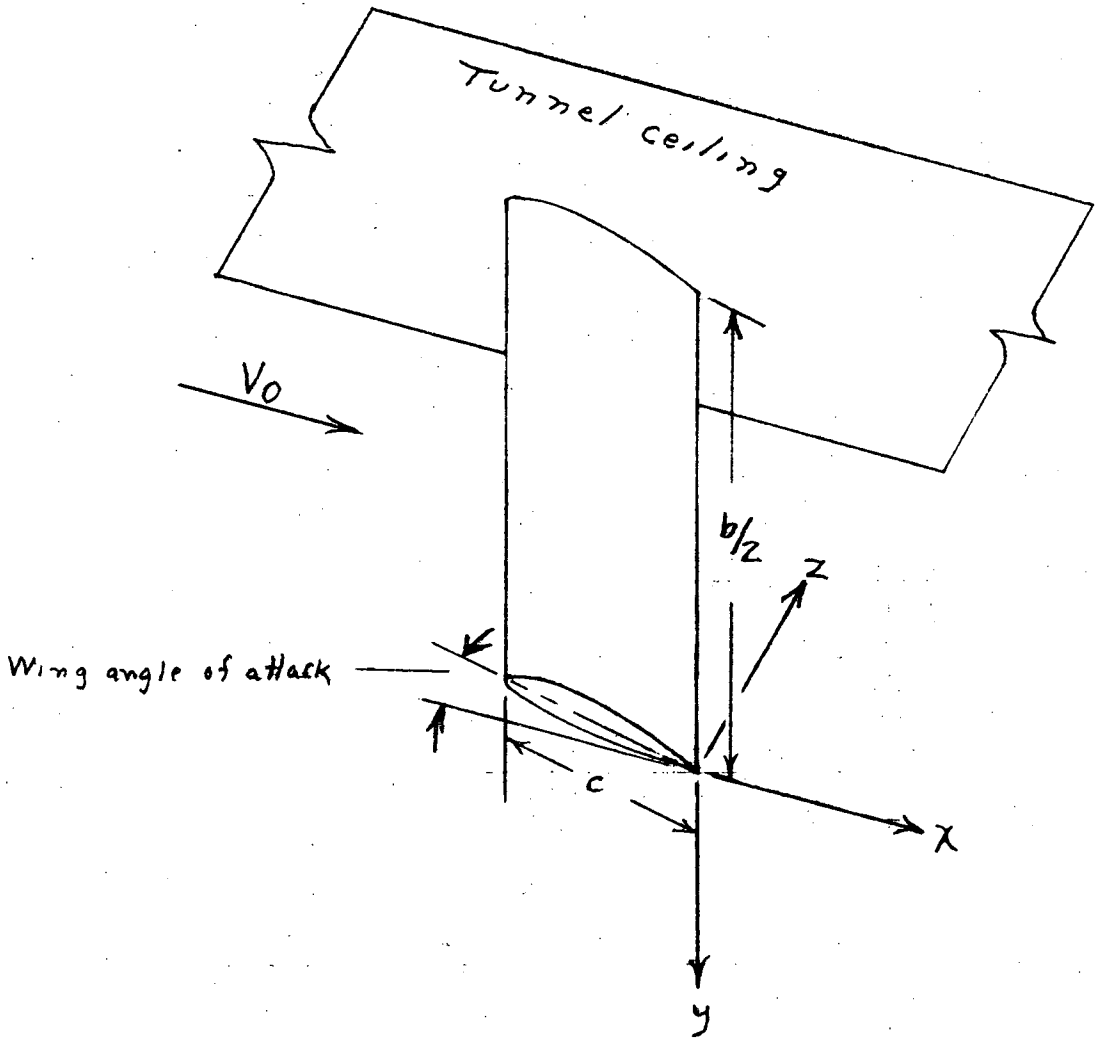

Figure 7.- Geometry and coordinate system.

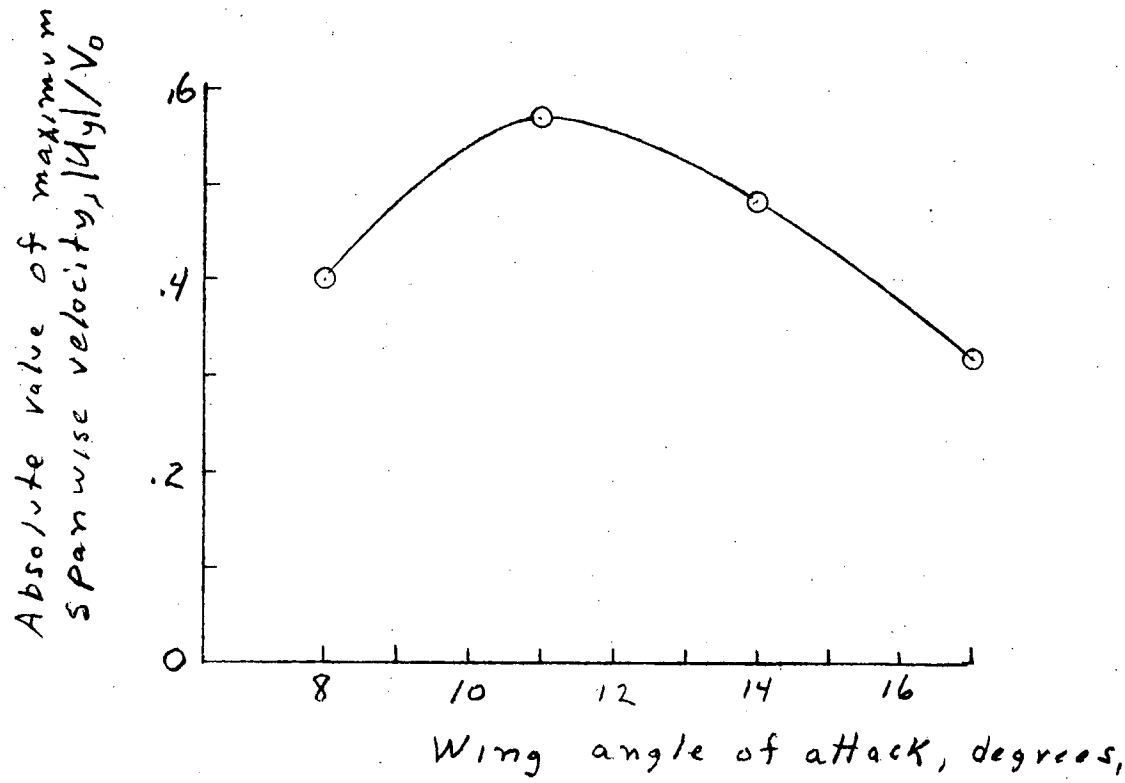

Figure 8.- Maximum spanwise velocity measured in the vortex as a function of wing angle of attack, x/c = 7.03.

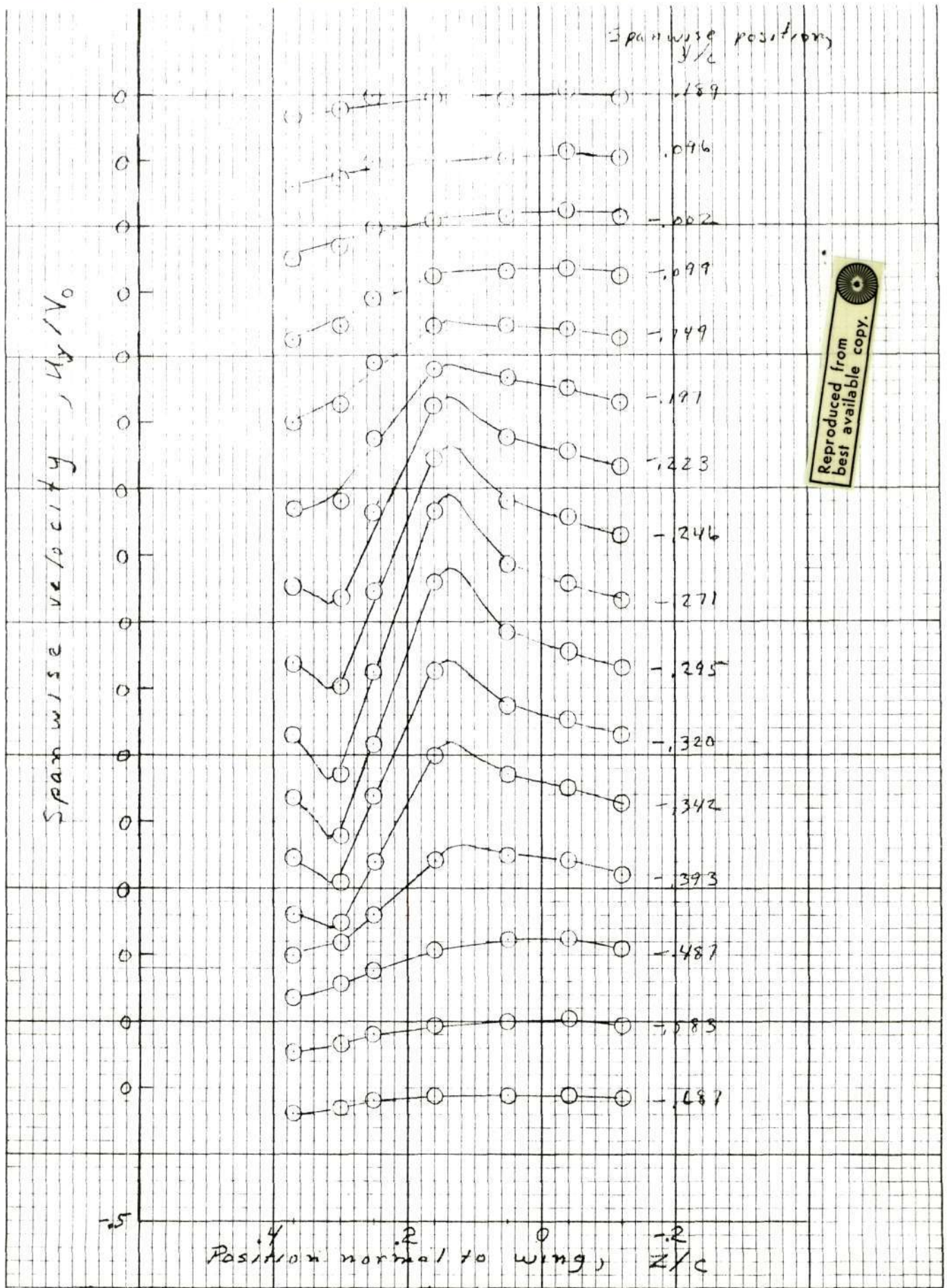

Figure 9.- Spanwise velocity profiles obtained by sweeping the flow angularity rake across the vortex path, $x/c = 7.03$.

	○ Present test	□ Rectangular wing of Ref. 2	△ Rectangular wing of Ref. 4	◇ Rectangular wing of Ref. 3
Air foil	(See fig.)	R.A.F. 6a	NACA 0009	NACA 0015
Semi-span	133.7 cm	91.5 cm	24.7 cm	121.8 cm
Tip Chord	26.3 cm	15.2 cm	7.6 cm	45.7 cm
Angle of attack	11°	6°	8°	12°
Estimated core diameter at $x/c \approx 7$	0.17c	0.15c	0.24c	0.10c

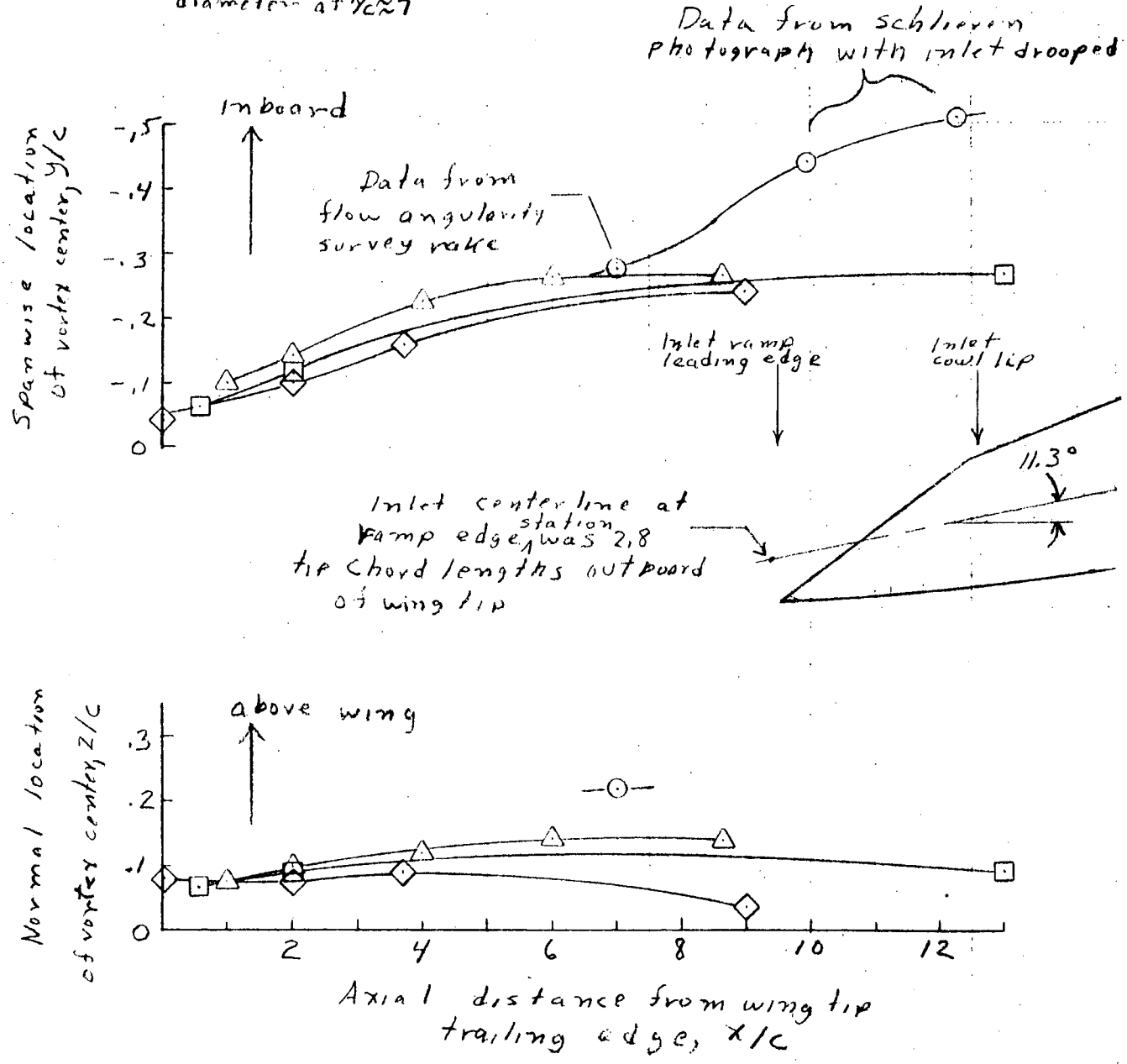

Figure 10. - Spanwise and normal location of vortex centerline as a function of axial distance.

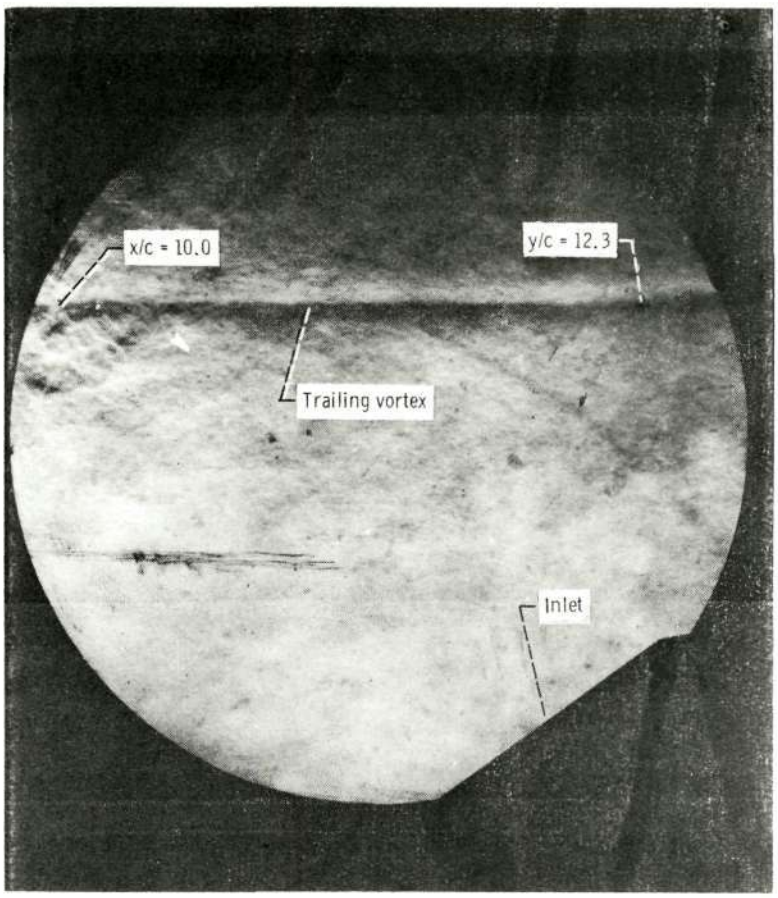

Figure 11. - Schlieren photograph of vortex trailing aft from wing tip, spanwise position of inlet centerline at ramp edge station, y/c = 2.8, inlet angle of attack, $\alpha = 11.3^{0}$.

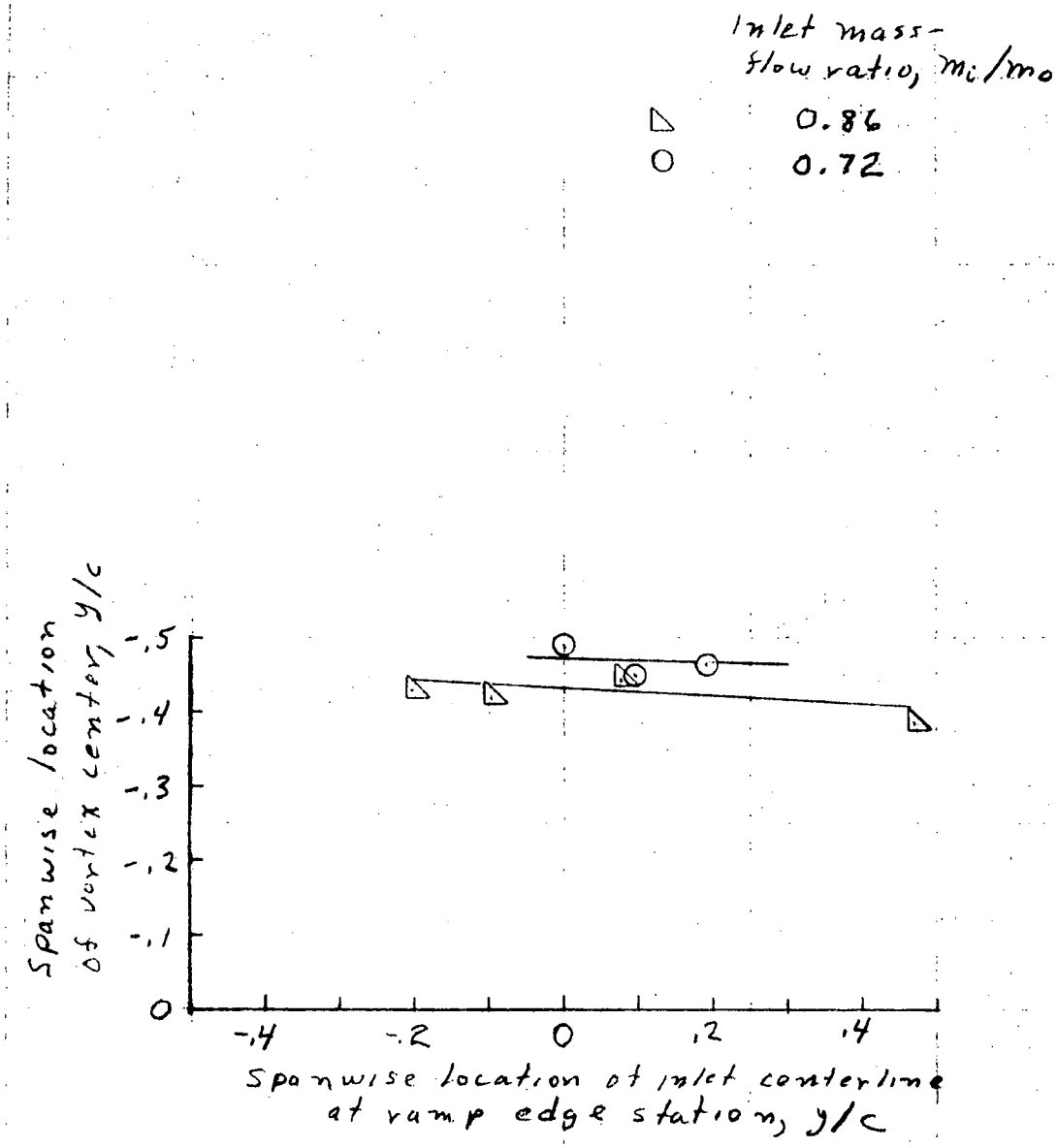

Figure 12. - Effect of spanwise inlet location on spanwise location of vortex at an axial location, x/c of 10.0.

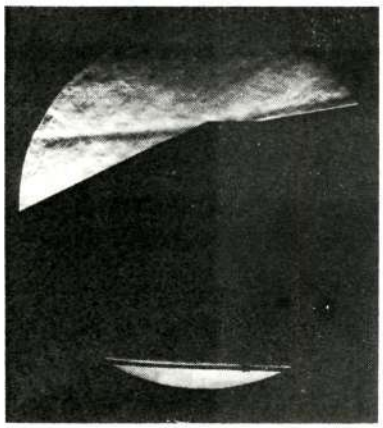

(a) Inlet mass-flow ratio, 0.72.

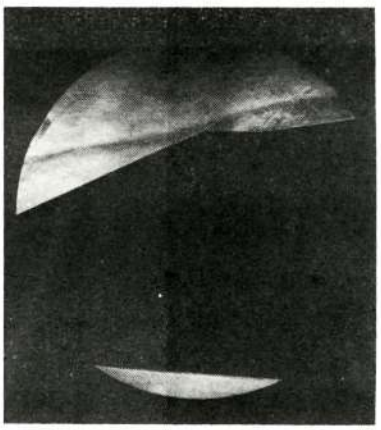

(b) Inlet mass-flow ratio, 0.61.

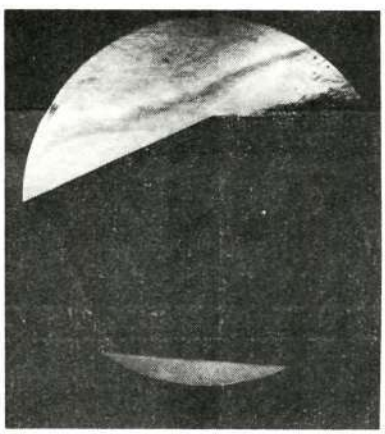

(c) Inlet mass-flow ratio, 0.30.

Figure 13. - Schlieren photographs showing effect of inlet mass-flow ratio on vortex path, spanwise position of inlet centerline at ramp edge station, y/c = 0.189, inlet angle of attack, $\alpha = -0.26^{0}$.

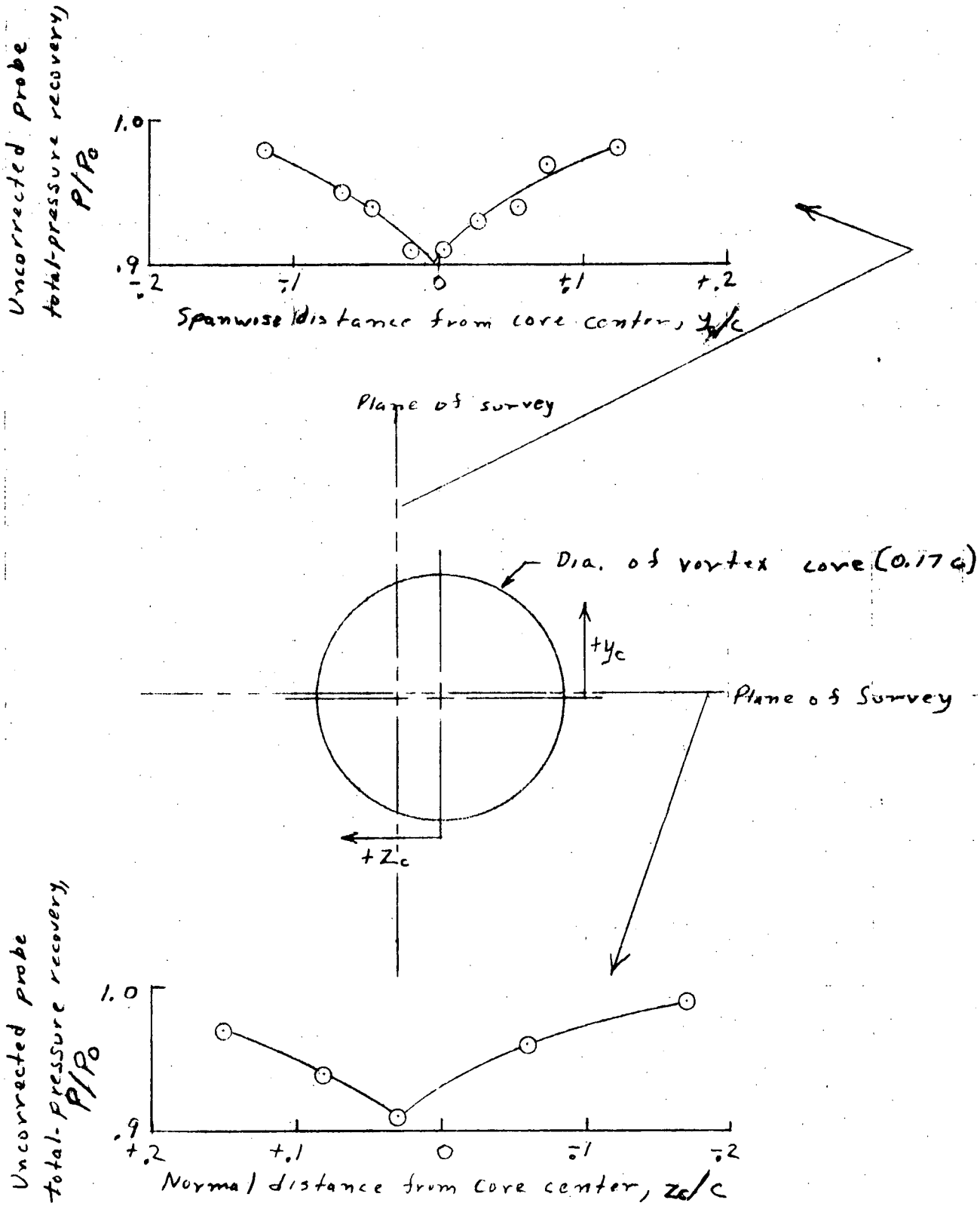

Figure 14. - Measured total-pressure profiles across the vortex core, x/c = 7.03.

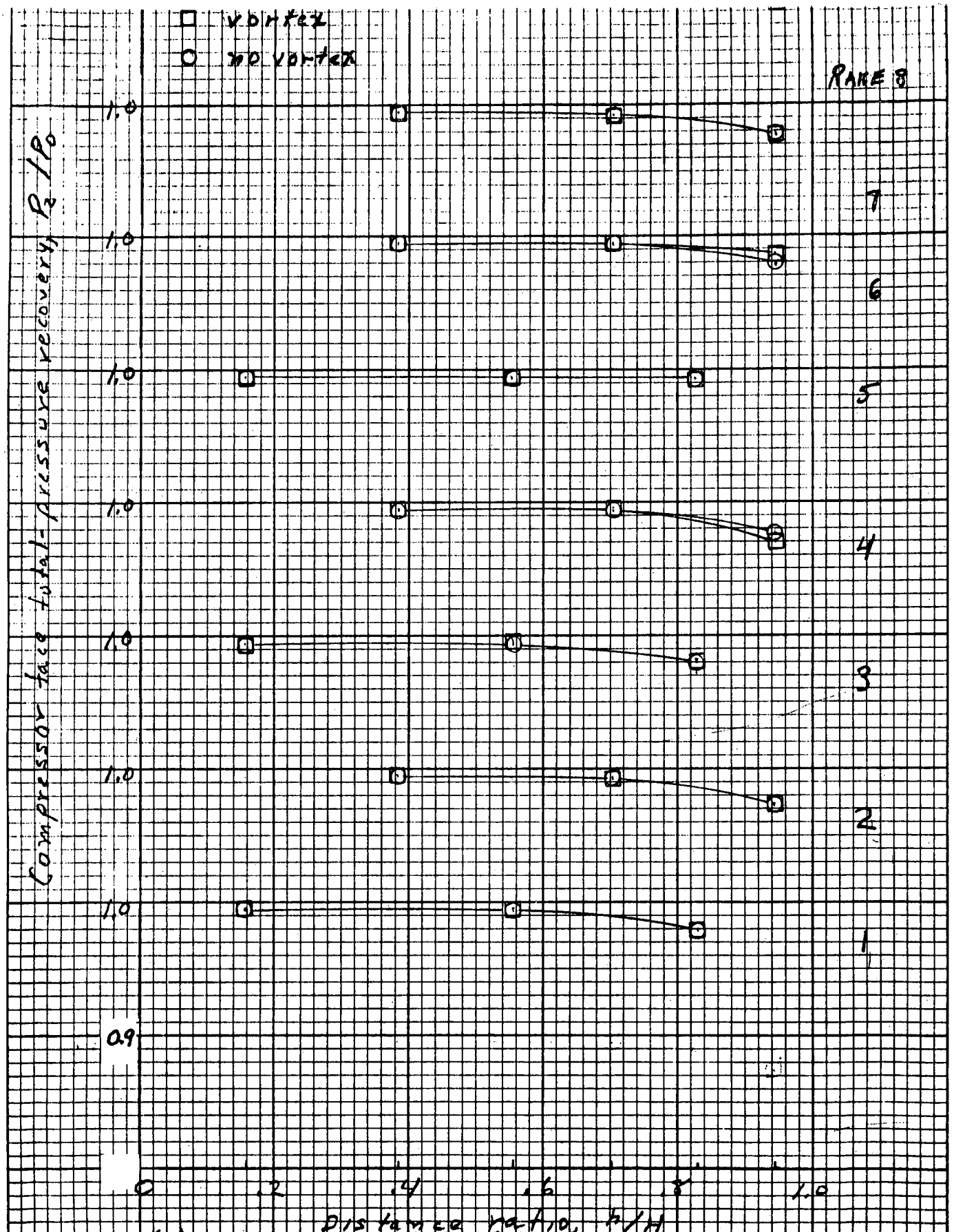

(a) Spanwise position of inlet centerline at ramp edge station, y/c = 0.189, inlet angle of attack, α =-0.26

Figure 15 - Effect of vortex on compressor-face total-pressure profiles at two spanwise inlet position. Inlet mass-flow ratio, M_i/M_0 = 0.63, x/c = 18.2.

(b) Spanwise position of inlet centerline at ramp edge station, y/c =-0.295, inlet angle of attack, α = -2.4°.

Figure 15 - Concluded.

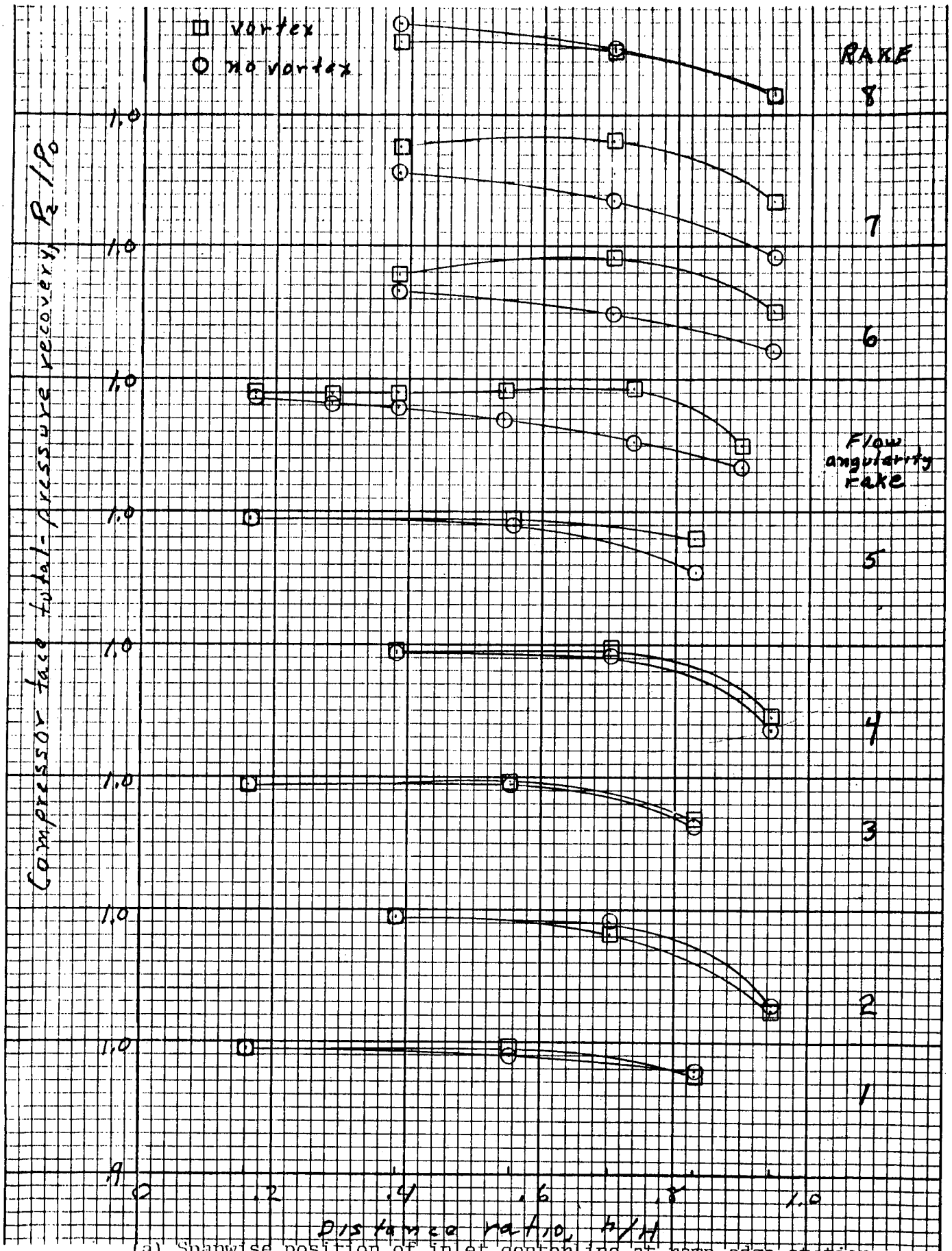

(a) Spanwise position of inlet centerline at ramp edge station, y/c = 0.474, inlet angle of attack, $\alpha = 1.0^{\circ}$.

Figure 16 - Effect of vortex on compressor-face total-pressure profiles at various spanwise inlet positions, inlet mass-flow ratio, M_i/M_0 = 0.86, x/c = 18.2

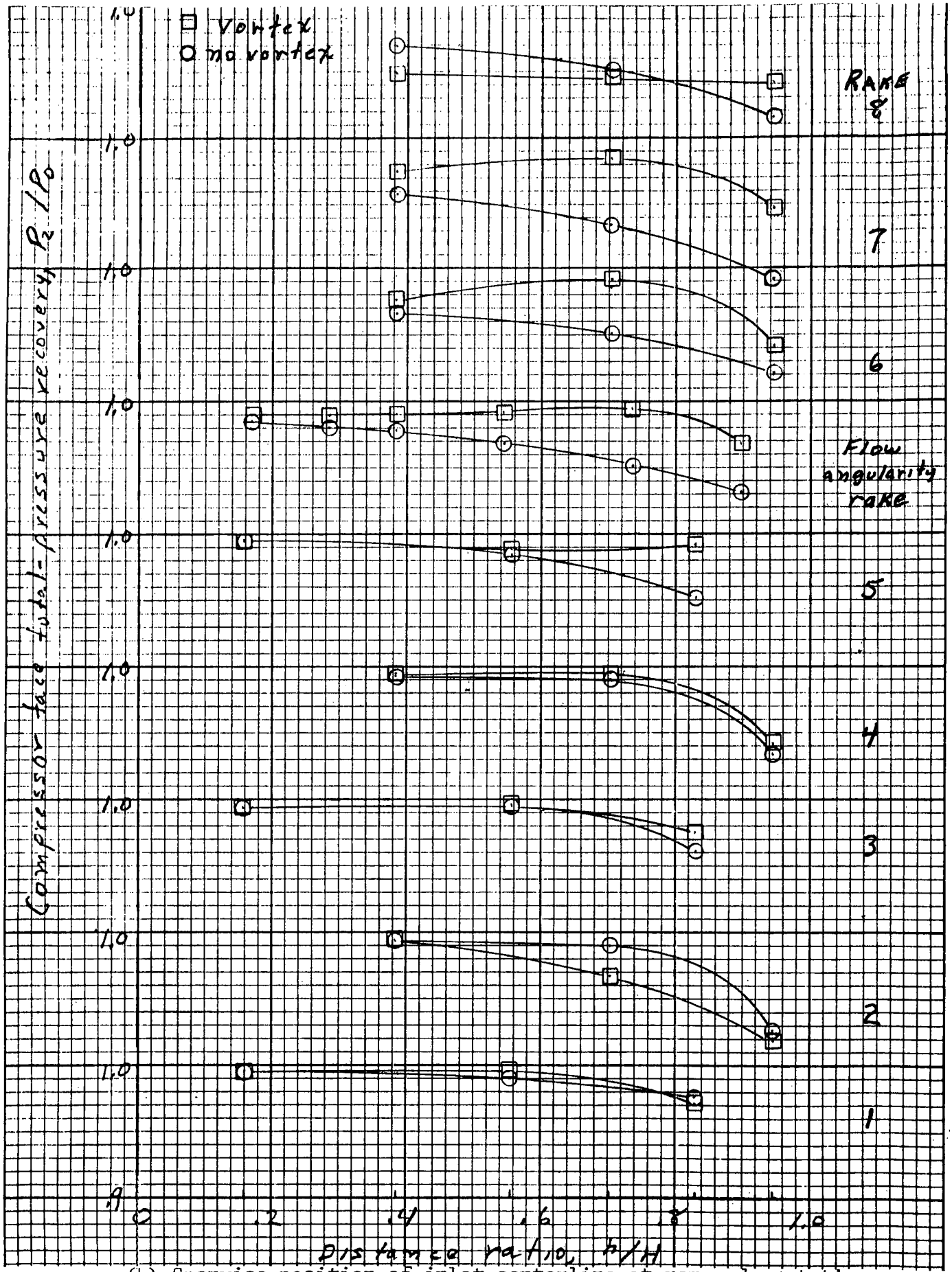

(b) Spanwise position of inlet centerline at ramp edge station, y/c = 0.291, inlet angle of attack, α = 0.2°.

Figure 16 - Continued.

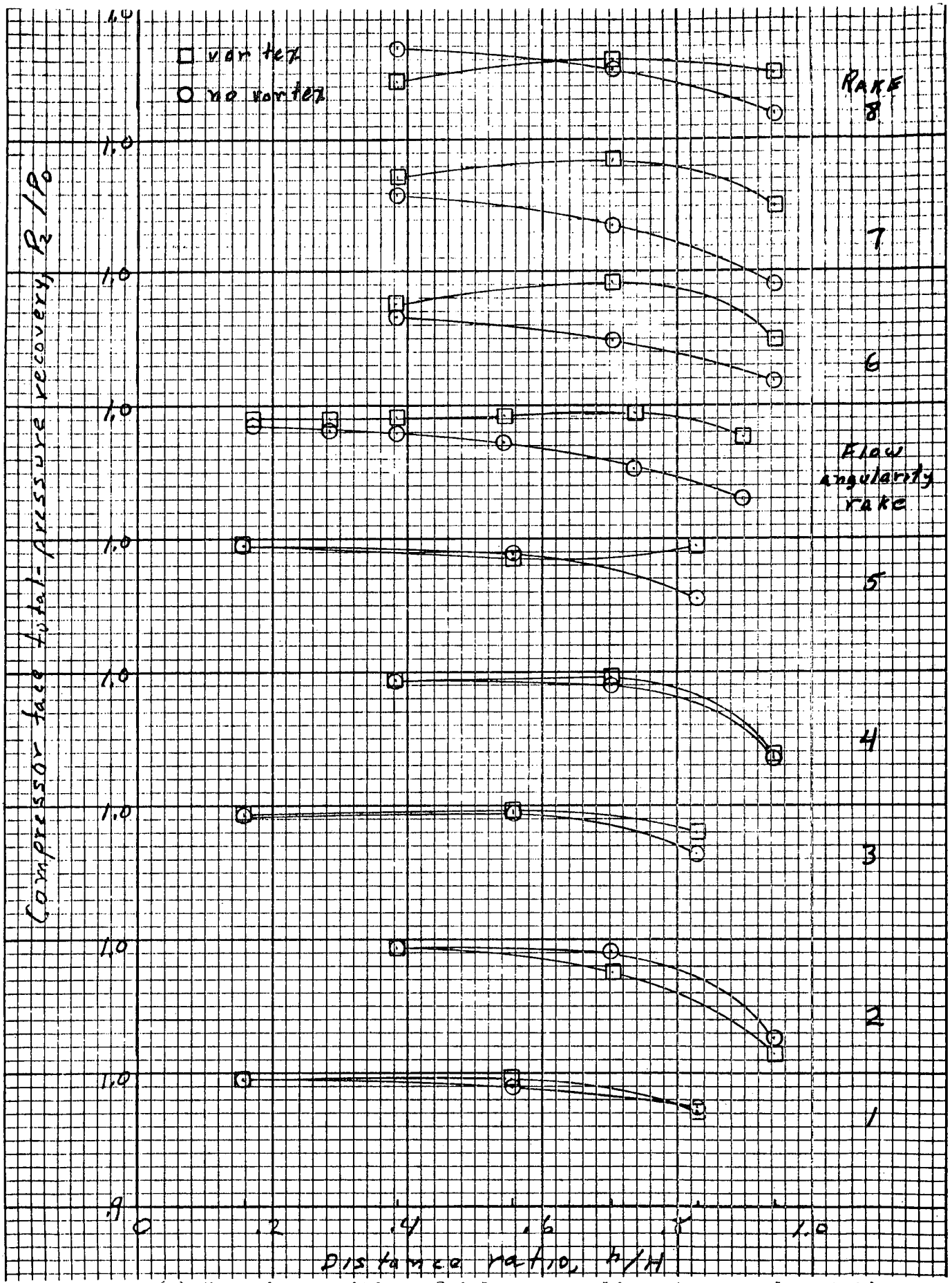

(c) Spanwise position of inlet centerline at ramp edge station, y/c = 0.189, inlet angle of attack, $\alpha = -0.26^{\circ}$.

Figure 16 - Continued.

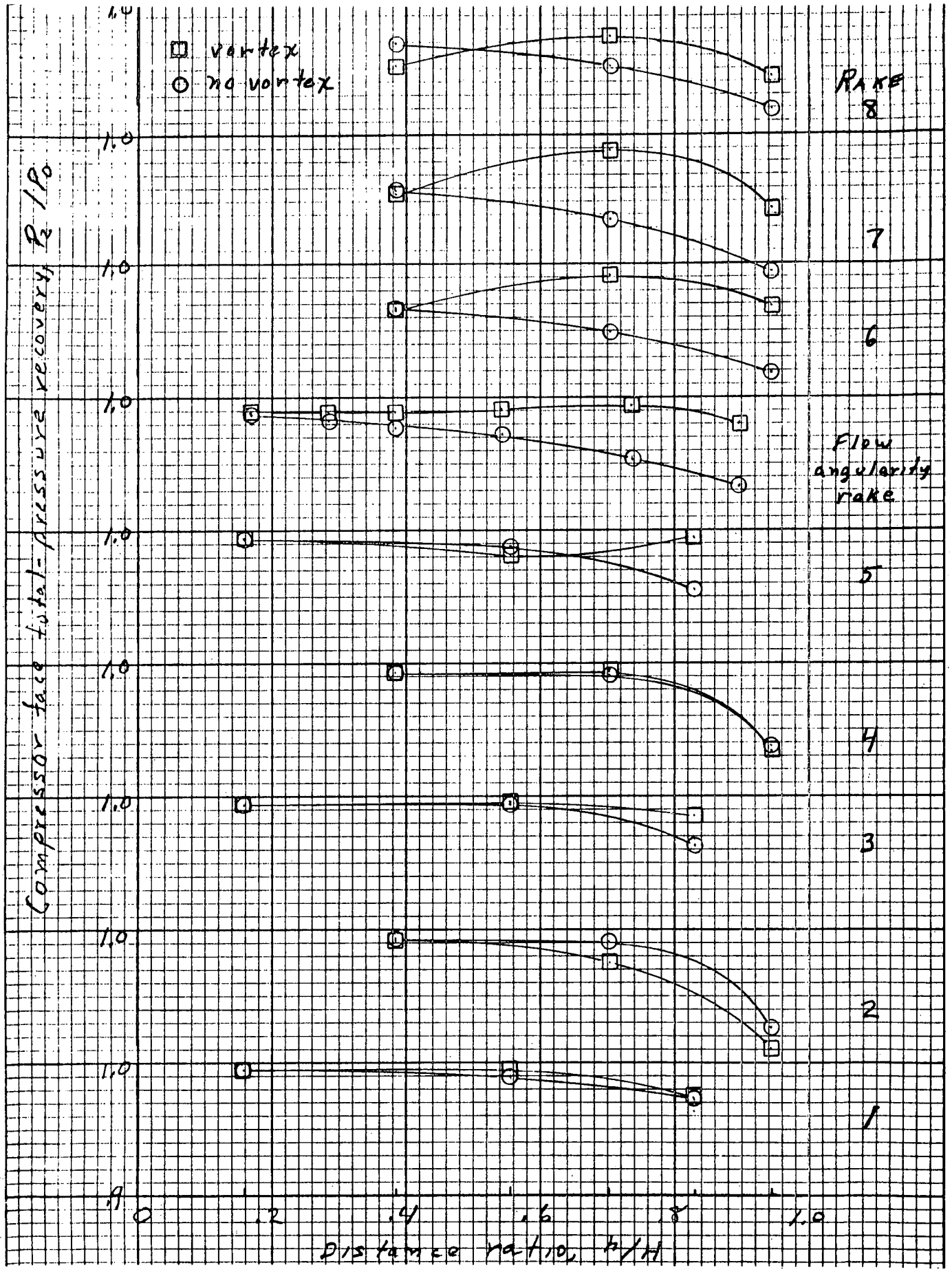

(d) Spanwise position of inlet centerline at ramp edge station, y/c = 0.077, inlet angle of attack, α =-0.75.

Figure 16 - Continued.

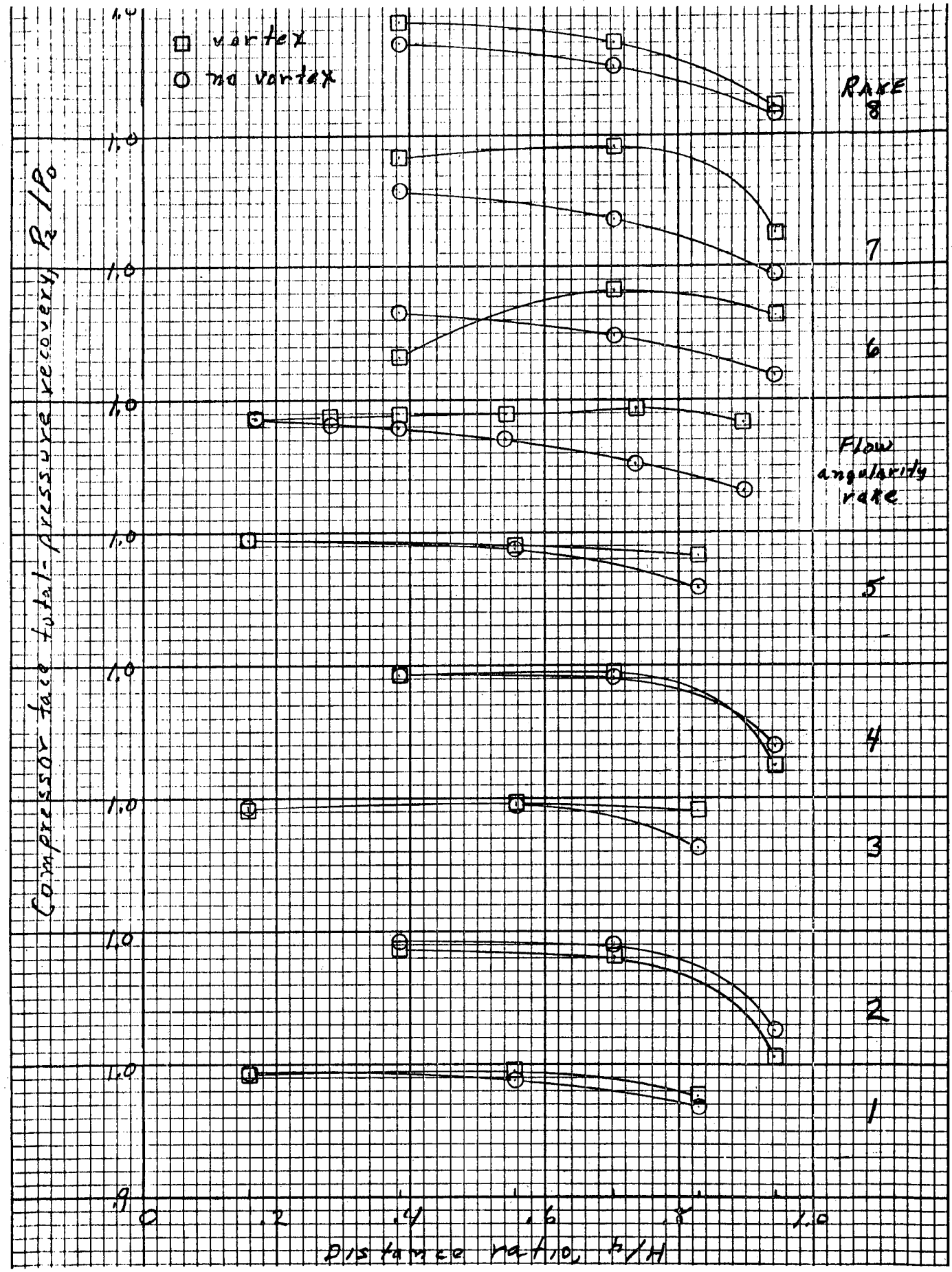

(e) Spanwise position of inlet centerline at ramp edge station, y/c =-0.095, inlet angle of attack, α =-1.5°.

Figure 16 - Continued.

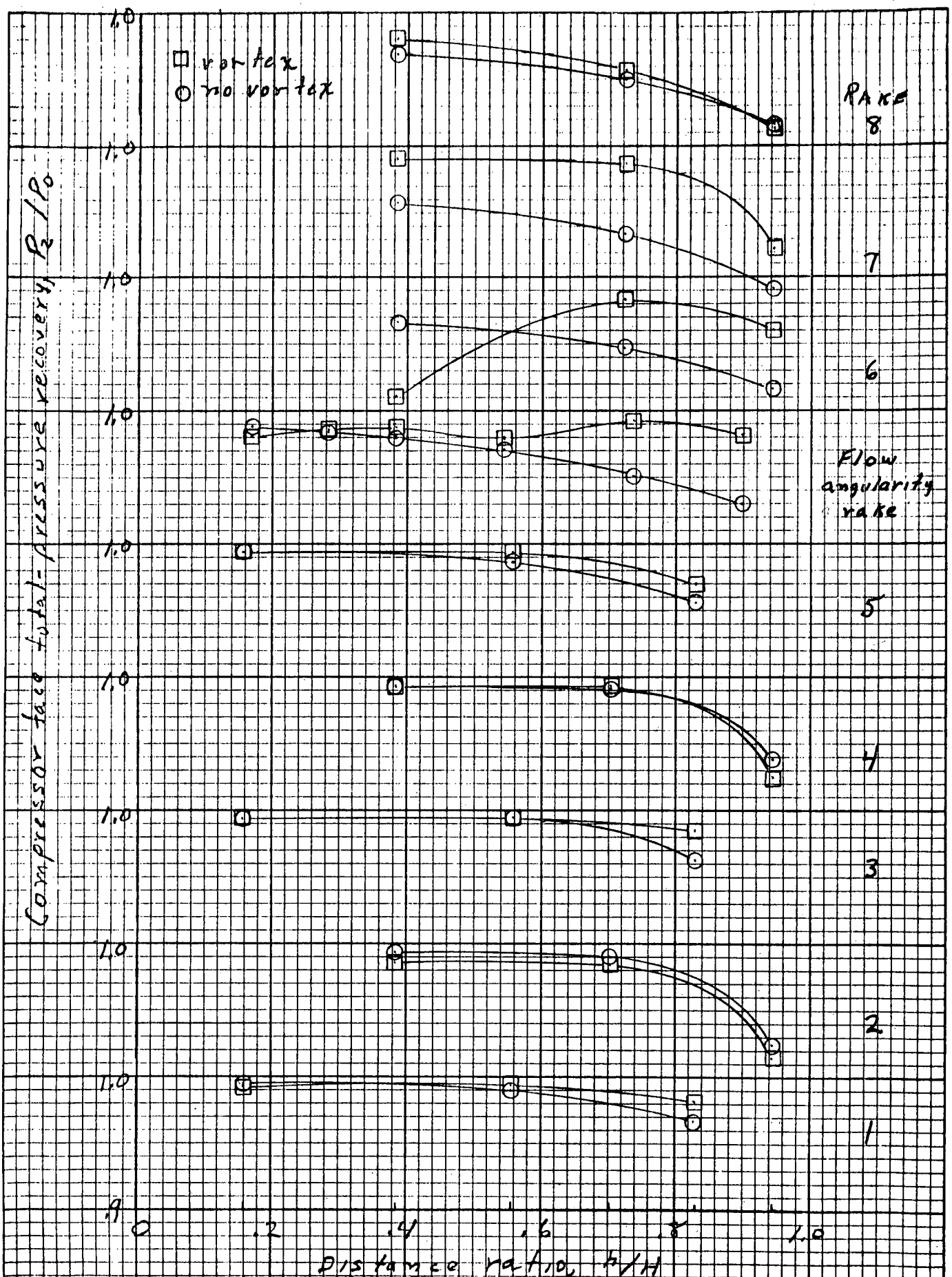

(f) Spanwise position of inlet centerline at ramp edge station, y/c =-0.207, inlet angle of attack, α =-2.0°.

Figure 16 - Continued.

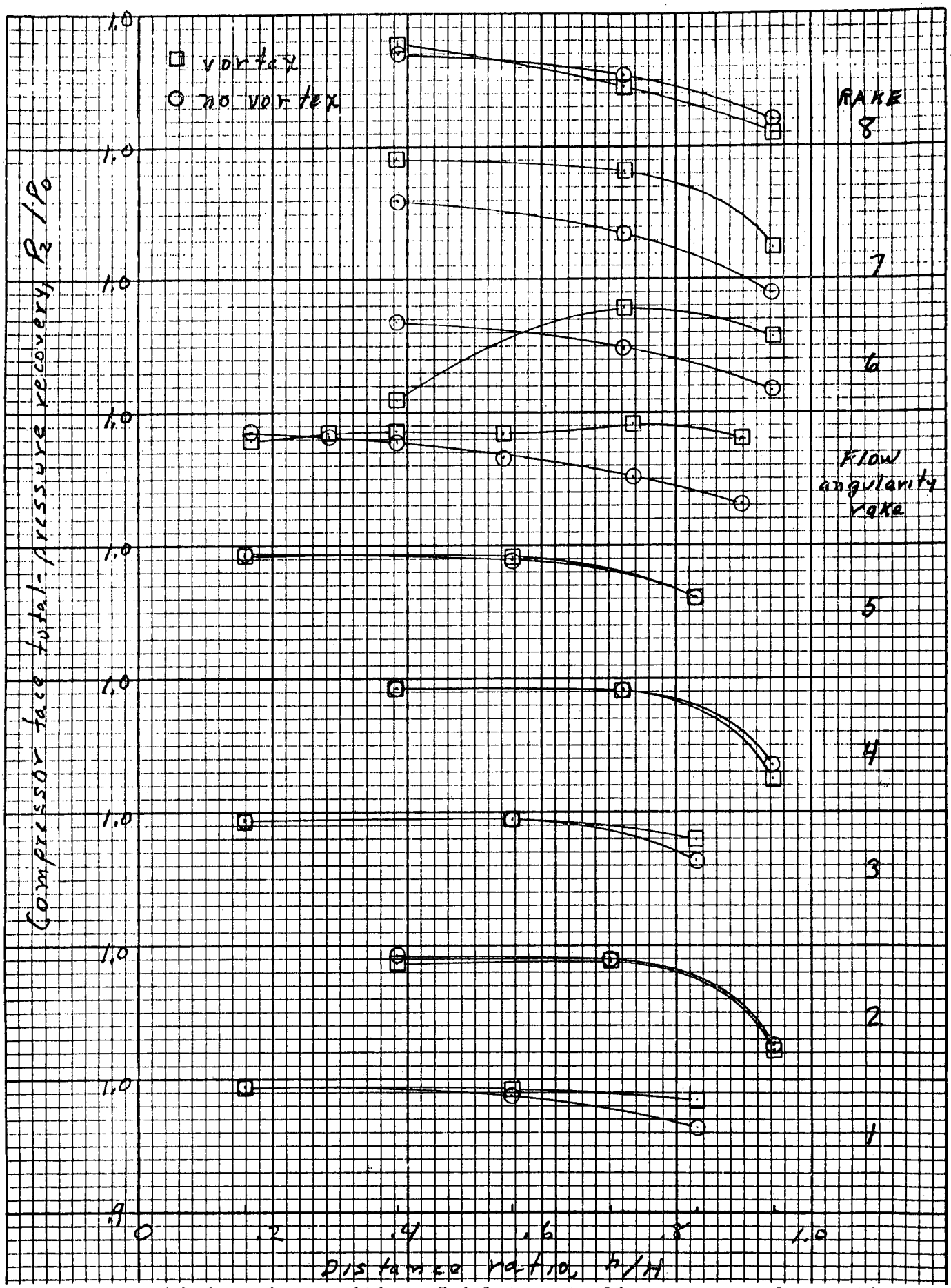

(g) Spanwise position of inlet centerline at ramp edge station, y/c =-0.295, inlet angle of attack, α=-2.4°.

Figure 16 - Continued.

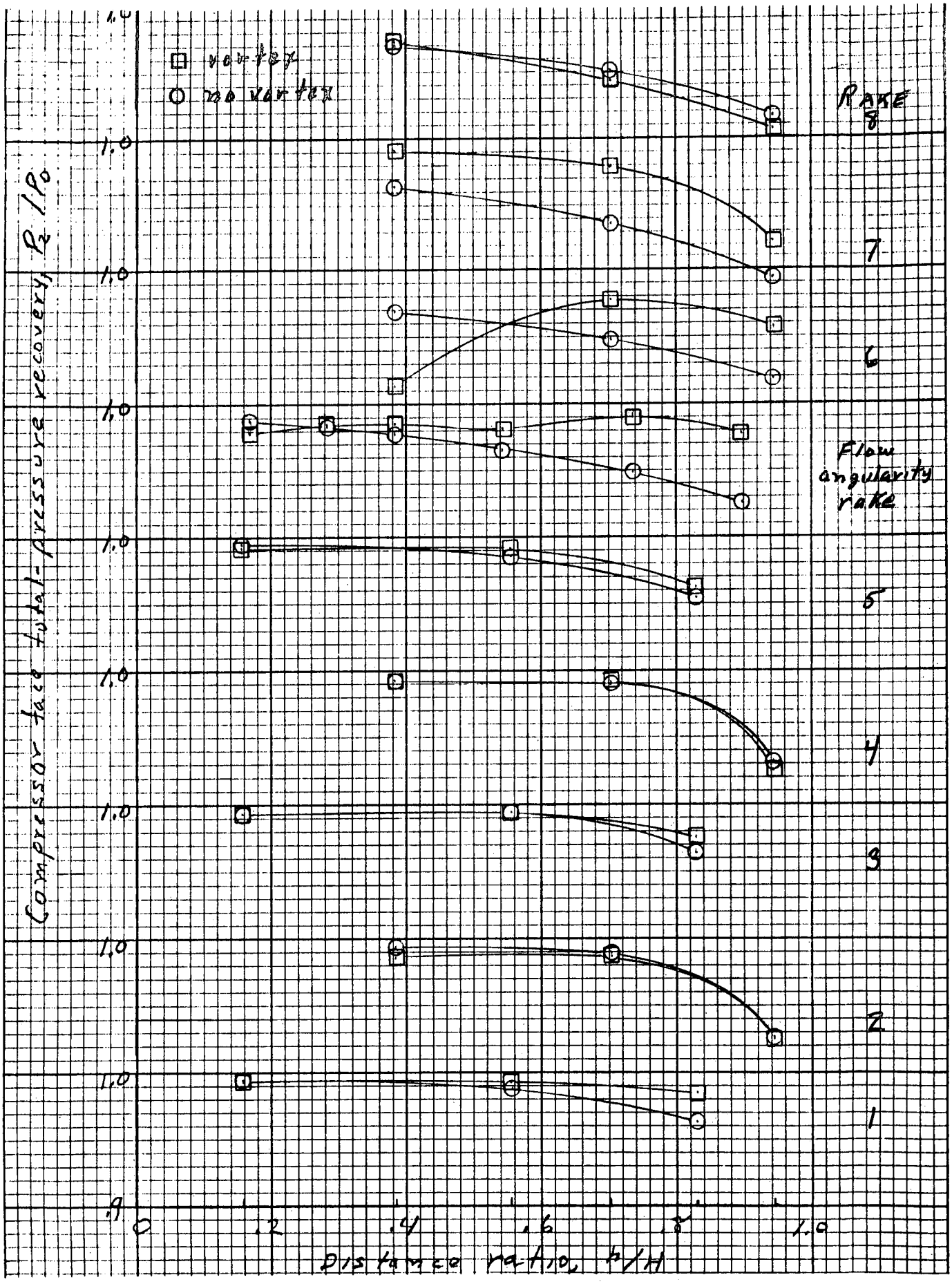

(h) Spanwise position of inlet centerline at ramp edge station, y/c =-0.320, inlet angle of attack, α=-2.5°.

Figure 16 - Continued.

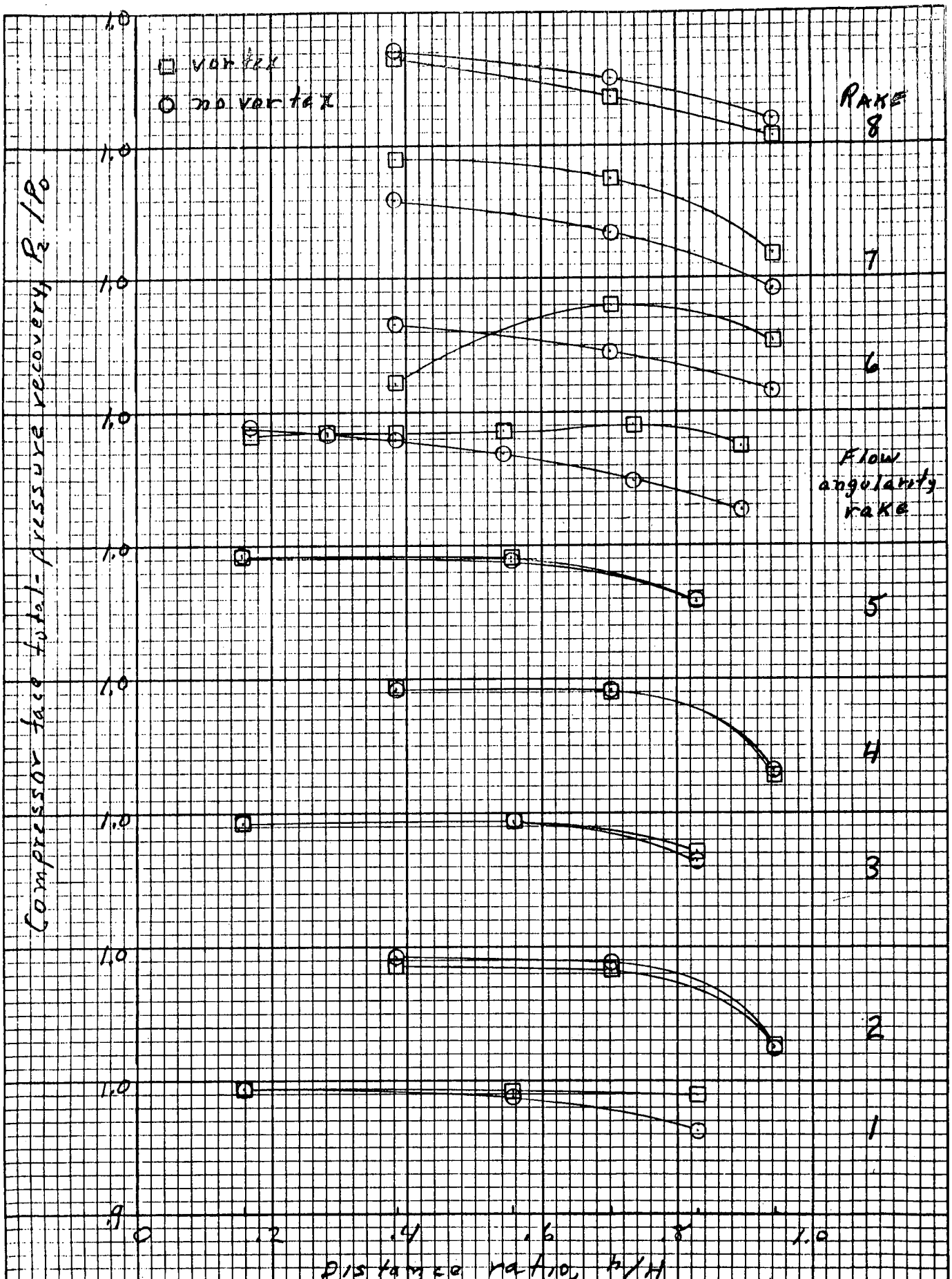

(i) Spanwise position of inlet centerline at ramp edge station, y/c =-0.376, inlet angle of attack, α=-2.75°.

Figure 16 - Continued.

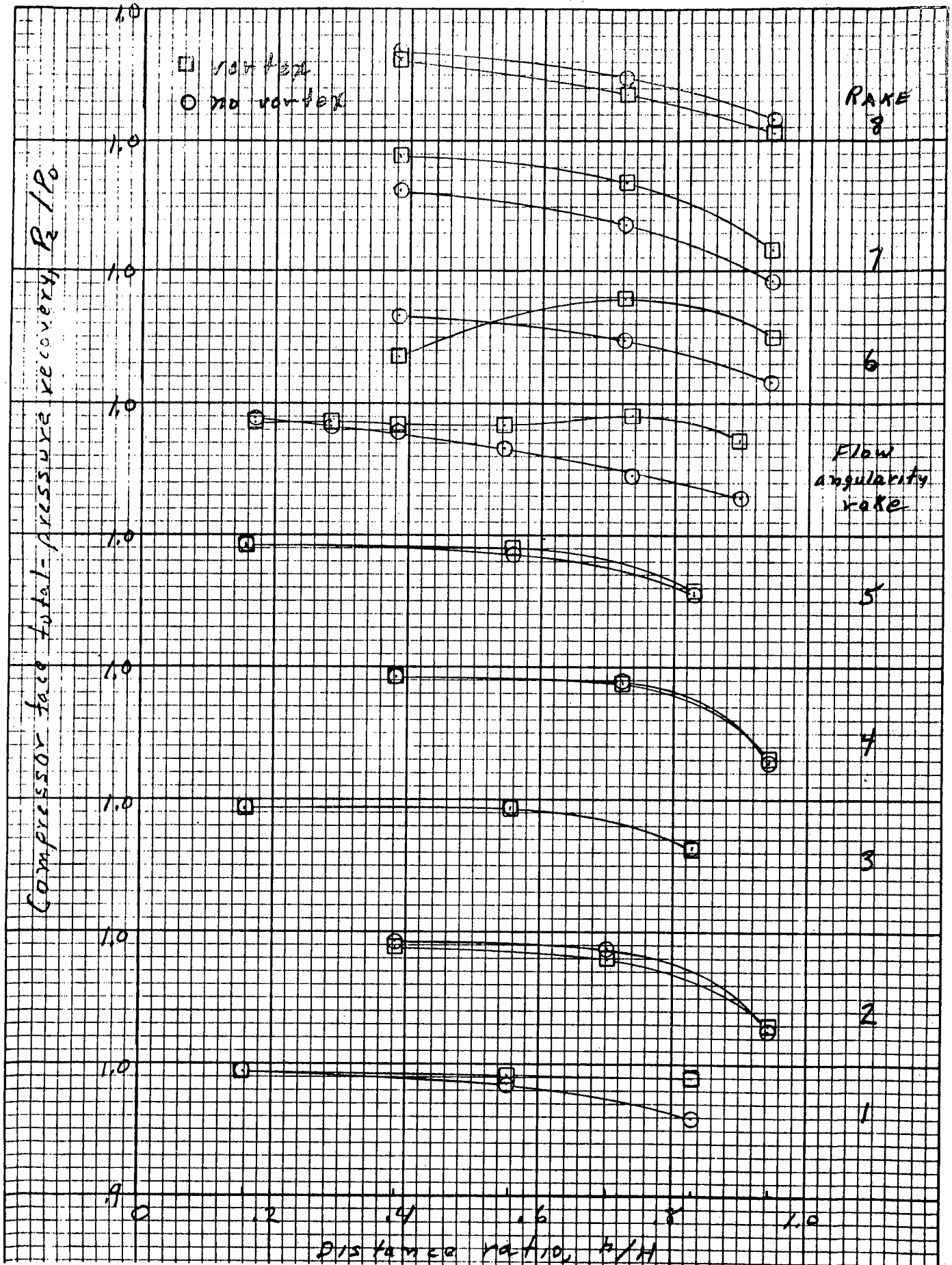

(j) Spanwise position of inlet centerline at ramp edge station, y/c =-0.433, inlet angle of attack, α=-3.0°.

Figure 16 - Concluded.

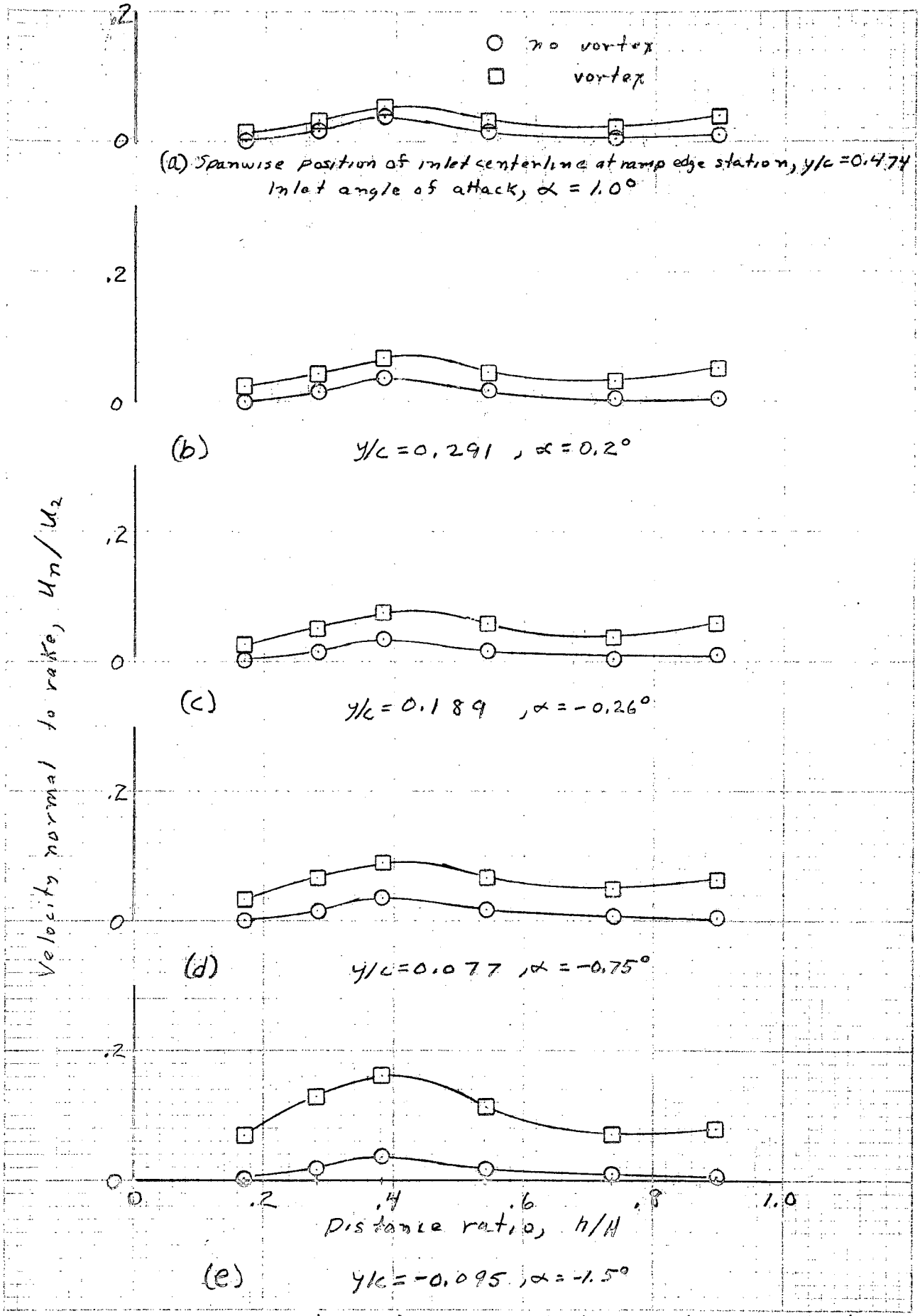

Figure 17.- Velocity profiles normal to the flow angularity rake mounted at the compressor face station, inlet mass-flow ratio, $m_i / m_o = 0.86$.

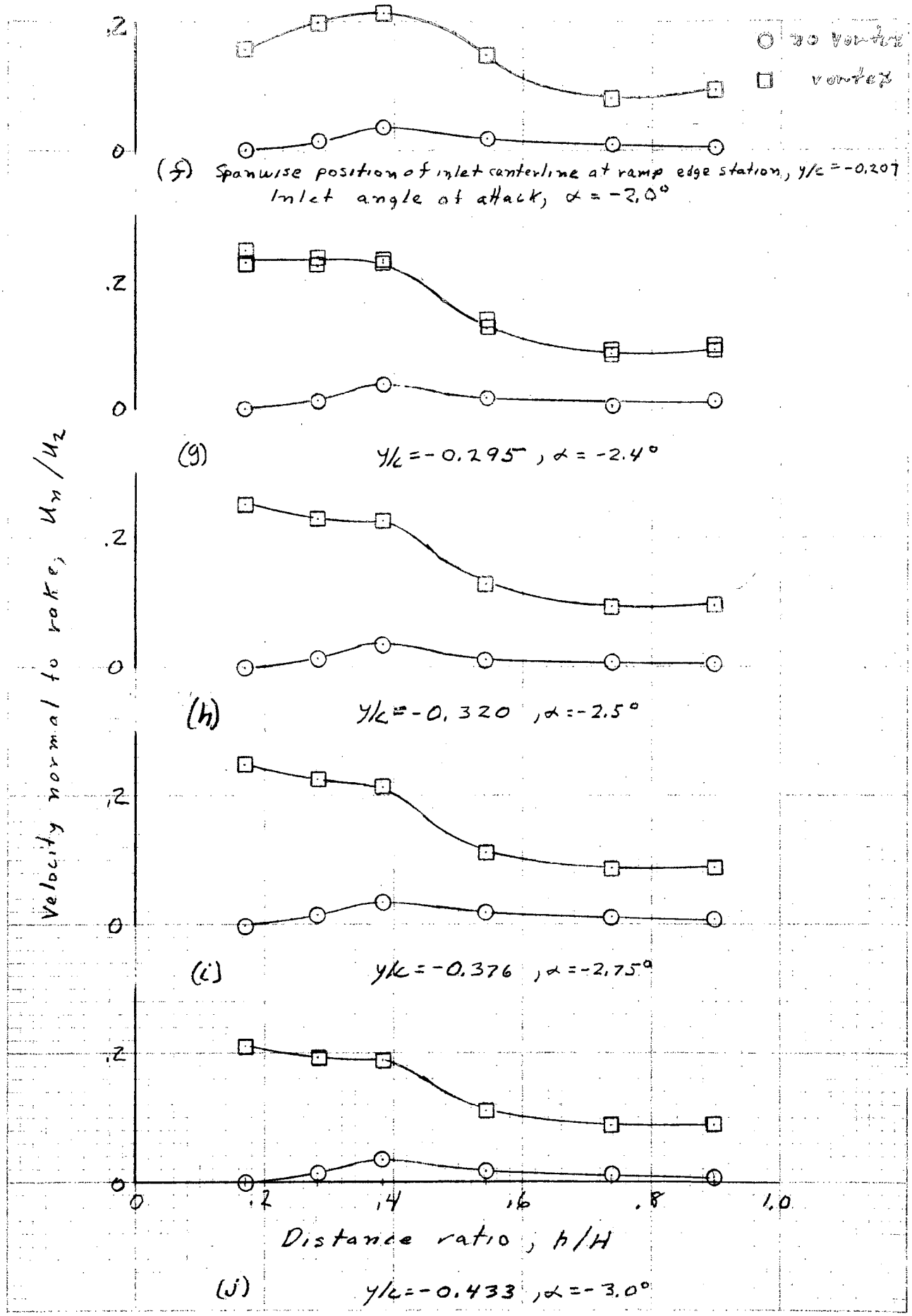

Figure 17.- Concluded.